University of Szeged
Faculty of Pharmacy
Doctoral School of Pharmaceutical Sciences
Institute of Pharmacognosy

# Studies on the scavengeome of resveratrol

**Ph.D. Thesis**

Orinamhe Godwin Agbadua

**Supervisor:**

Attila Hunyadi, DSc

Szeged, Hungary
2025

## LIST OF PUBLICATIONS RELATED TO THE THESIS*

This thesis is based on the following publications:

I. **Agbadua, O.G**., Kúsz, N., Berkecz, R., Gáti, T., Tóth, G., Hunyadi, A. (2022). Oxidized Resveratrol Metabolites as Potent Antioxidants and Xanthine Oxidase Inhibitors. *Antioxidants*, *11*, 1832. IF6.6 (D1)

II. **Agbadua, O.G**., Kúsz, N., Berkecz, R., Vass, E., Csámpai, A., Tóth, G., Balogh, G.T., Marcourt, L., Wolfender, J., Queiroz, E.F., Attila Hunyadi, A. (2025). New Insights into the French Paradox: Free Radical Scavenging by Resveratrol Yields Cardiovascular Protective Metabolites.
*Journal of Medicinal Chemistry*, *68* (10), 10031-10047 IF 6.8 (D1)

## OTHER PUBLICATIONS RELATED TO THE TOPIC OF THE THESIS

I. Hunyadi, A., **Agbadua, O. G**., Takács, G., Balogh, G. T. (2023). Scavengome of an Antioxidant.
I*n Vitamins and Hormones*, Litwack, G., Ed.; Academic Press: Cambridge, MA, USA, Volume 121, pp. 81–108. IF 2.7 (Q2)

*: Latin numerals of the corresponding publications related to the thesis will be reference in this dissertation.

**LIST OF ABBREVIATIONS**

| | |
|---|---|
| $^{\bullet}OH$ | Hydroxyl radical |
| µL | Microliter |
| $^{13}C$ NMR | Carbon nuclear magnetic resonance |
| $^{1}H$ NMR | Proton nuclear magnetic resonance |
| AAPH | 2,2'-Azobis(2-amidinopropane) dihydrochloride |
| Abz- LFK(Dnp)-OH | 2-Aminobenzoyl-Leucine-Phenylalanine-Lysine(Dinitrophenyl)-Hydroxyl |
| Abz-SDK(Dnp)P-OH | 2-Aminobenzoyl-Serine-Aspartate-Lysine(Dinitrophenyl)-Pro-Hydroxyl |
| ACD | Advanced Chemistry Development |
| ACE | Angiotensin converting enzyme |
| AIBN | Azobisisobutyronitrile |
| APT | Attached proton test ($^{13}C$-NMR) |
| aq. | Aqueous |
| BPPb | Bradykinin potentiating peptide B |
| C-ACE | ACE C-terminal domain |
| CAD | Charged aerosol detection |
| CAT | Catalase |
| $CH_3CN$ | Acetonitrile |
| $CH_3OH$ | Methanol |
| COX-1 | Cyclooxygenase-1 |
| COX-2 | Cyclooxygenase-2 |
| CVDs | Cardiovascular diseases |
| CyP1A2 | Cytochrome P450 1A2 |
| DMSO | Dimethyl sulfoxide |
| DPPH | 1, 1-Diphenyl-2-picrylhydrazyl |
| ELSD | Evaporative Light Scattering Detector |
| equiv | Equivalent |
| EtOH | Ethanol |
| Ex/Em | Extinction/emission |
| GSH | Reduced glutathione |
| $H_2O$ | Water |
| $H_2O_2$ | Hydrogen peroxide |
| HMBC | Heteronuclear Multiple Bond Correlation |
| HPLC | High-performance liquid chromatography |
| HRMS | High-resolution mass spectroscopy |
| HSQC | Heteronuclear single quantum correlation |
| IC50 | Fifty percent inhibitory concentration |
| IEF-PCM | integral equation formalism-polarizable continuum model |
| Inh. | Inhibition |
| Kcal | Kilocalorie |

| | |
|---|---|
| $K_M$ | Michaelis constant |
| LA-REIMS | Laser-assisted rapid evaporative ionization mass spectrometry |
| LLE | Ligand-lipophilicity efficiency |
| log$D_{7.4}$ | Logarithm of the distribution coefficient at pH 7.4 |
| 15-LOX | 15-Lipoxygenase |
| mg | Milligram |
| mL | Milliliter |
| mM | Millimolar |
| mU | Milliunit |
| N-ACE | ACE N-terminal |
| $O_2^{\bullet-}$ | Superoxide anion radical |
| $ONOO^-$ | Peroxynitrite |
| NOESY | Nuclear Overhauser Effect Spectroscopy |
| PCM | Polarizable continuum model |
| PDB | Protein Data Bank |
| PDBQT | Protein data bank, AutoDock format |
| PIDA | Iodobenzene diacetate |
| PIFA | Iodobenzene bis(trifluoroacetate) |
| Ox | Oxidized |
| PDA | Photodiode array |
| ROS | Reactive oxygen species |
| RNS | Reactive nitrogen species |
| RP-HPLC | Reverse-phase high pressure liquid chromatography |
| SAR | Structure-activity relationship |
| SEM | Standard error of the mean |
| SOD | Superoxide dismutase |
| TPSA | Topological polar surface area |
| $TxA_2$ | Thromboxane A2 |
| $V_{MAX}$ | Maximal velocity |
| UV | Ultraviolet |
| VCD | Vibrational circular dichroism |
| XO | Xanthine oxidase. |

**Table of Contents**

## 1.0 INTRODUCTION

### 1.1 Free radicals; types and sources

Free radicals have gained increasing significance due to their central role in physiological signaling and pathological processes in various biological systems.[1,2] Free radicals, which include various oxygen- or nitrogen-centered radicals, collectively called reactive oxygen and nitrogen species (RONS), are derived from both endogenous and exogenous sources.[2,3] Key endogenous sources of reactive oxygen species (ROS) include mitochondria, phagocytic cells, peroxisomes, and the endoplasmic reticulum, along with several oxidative enzymes such as NADPH oxidase, xanthine oxidase, and NO synthase.[4] Among these, mitochondrial electron transport chain enzymes remain the most significant contributor to most intracellularly derived ROS.[1,5] The most biologically relevant ROS include hydrogen peroxide ($H_2O_2$), superoxide anion radical ($O_2^{\bullet-}$), singlet oxygen ($^1O_2$), hypochlorous acid (HOCl), hydroxyl radical (•OH), alkoxyl (RO•), and peroxyl radicals (ROO•).[6-10] Meanwhile, the key reactive nitrogen species (RNS) are nitric oxide (NO), nitrogen dioxide ($NO_2$), and peroxynitrite ($ONOO^-$).[11,12] Furthermore, transition metals such as iron and copper are integral to the generation of free radical, facilitating the production of hydroxyl radical via Fenton and Fenton-like reactions.[13]

### 1.2 Antioxidants and oxidative stress

Low or moderate levels of RONS play essential physiological roles, including pathogen defense by the immune system, regulation of systemic circulation, and mediation of intracellular signaling pathways.[2] Notably, ROS can protect cells against oxidative damage by inducing antioxidant defense mechanisms and maintaining redox homeostasis.[14,15] Maintaining a balanced redox state is critical for homeostatic cellular activities, since fluctuations in redox status significantly influence transcriptional activity and signaling pathways regulated by oxidation-reduction processes.

Antioxidant enzymes counteract the potentially harmful effects of RONS, and oxidative stress occurs when an imbalance between these free radicals and antioxidants occurs due to depletion of antioxidants or ROS accumulation.[16] This imbalance leads to biomolecular damage, including lipid peroxidation, protein oxidation, and DNA damage, ultimately contributing to the development of various diseases such as cardiovascular diseases (CVDs) and cancer.[14,17] Naturally, biological systems are equipped with several antioxidant defense mechanisms that

counterbalance the effect of oxidants. Antioxidants function through diverse mechanism, including neutralizing oxidants by donating or accepting electron(s), breaking free radical chain reactions, inhibiting lipid peroxidation, or repairing oxidative damage to biomolecules.[14,18] The human body possesses an excellent intrinsic antioxidant system, complemented by exogenous antioxidants from dietary sources such as fruits, vegetables, herbs and spices, all mostly rich in polyphenols.[19] Antioxidants are broadly classified into enzymatic antioxidants like superoxide dismutase (SOD), catalase (CAT), glutathione peroxidase (GPx), thioredoxin, peroxiredoxin (PRX) and glutathione transferase (GST), and nonenzymatic antioxidants such as vitamin A, ascorbic acid, α-tocopherol, β-carotene and glutathione. Collectively, these antioxidants play unique roles in maintaining RONS at physiologically optimal levels.[20]

### 1.3 Polyphenols as dietary antioxidants

Polyphenols are the largest and most studied group of naturally occurring antioxidants, characterized by hydroxyl group(s) attached to carbon atom(s) on an aromatic ring.[21] As exogenous antioxidants, it is widely established that polyphenols mitigate oxidative stress primarily by modulating signaling pathways that regulate oxidative balance, upregulating antioxidant defense mechanisms and downregulating pathways that increase free radical levels.[3,22]

Polyphenols enhance cellular antioxidant activity by modulating redox-sensitive transcription factors, primarily the nuclear factor erythroid 2-related factor 2 (Nrf2) - antioxidant-response elements (AREs) pathway, a key regulator of oxidative stress responses.[2,23] Under normal conditions, Nrf2 is sequestered by Keap1, which promotes its degradation, but oxidative stress induces Keap1 modifications, allowing Nrf2 nuclear translocation and activation of genes encoding antioxidant and detoxifying enzymes such as SOD, GPx1, GST, NQO1, HO-1, and TrxR.[23] Furthermore, polyphenols enhance the glutathione (GSH) redox system by increasing γ-glutamylcysteine synthetase (γ-GCS) activity, promoting GSH synthesis,[23] and activate the AMPK pathway, leading to upregulation of Mn-SOD and catalase.[24] In addition to stimulating antioxidant defenses, polyphenols contribute to downregulating the production and activity of pro-oxidative enzymes like NADPH oxidase, xanthine oxidase (XO), lipoxygenase (LOX), monoamine oxidase (MAO), and inducible nitric oxide synthase (iNOS).[25]

However, while thought to have little *in vivo* relevance in decreasing ROS/RNS levels, these antioxidants can also directly scavenge these free radicals by accepting or donating electron(s) due to the presence of aromatic rings, multiple hydroxyl groups, and a highly conjugated system.[26,27]

### 1.4 Scaveng(e)ome of dietary antioxidants

The term 'scaveng(e)ome' refers to the chemical space of all the metabolites that may be formed from an antioxidant upon scavenging ROS/RNS.[28,29] When free radicals are scavenged, the resulting reactive intermediate(s) may undergo redox cycling or become stabilized via intra- or intermolecular rearrangements. This can take place through many different chemical routes, therefore the formation of stable metabolites expectably leads to a structurally diverse array of small-molecule metabolites, frequently representing a greater chemical complexity relative to the parent antioxidant.[29] In biological systems, the specific types and quantities of ROS/RNS, dictated by localized oxidative stress conditions, play a crucial role in directing the metabolic fates of antioxidants. Although certain antioxidants, such as curcumin, can undergo oxidative fragmentation,[30] it is more common for free radical scavenging by an antioxidant to result in more complex chemical structures via radical coupling reactions, resulting in unique new rings or ring systems.[29]

These complex oxidized metabolites often exhibit modulated pharmacological activities compared to their parent compounds due to their increased molecular specificity when interacting with macromolecules.[28] A notable example of the biological relevance of a compound emerging from RONS scavenging by an antioxidant is vitamin C, which exhibits dual regulatory effects on NF-κB signaling: while its reduced form (ascorbic acid) scavenges ROS and decreases IκBα Kinase β (IKKβ) activation, its oxidized derivative (dehydroascorbic acid) selectively inhibits IKKβ, demonstrating a distinct pharmacological role.[31] Similarly, oxidized polyphenol metabolites may result in the formation of biologically active compounds on new bioactive targets that were previously inactive to the parent compound. One of such studies reported that biomimetic, Fe-catalyzed oxidation of resveratrol led to a mixture containing a variety of minor products that had potent LOX inhibitory activity in contrast to resveratrol, which was inactive.[32]

The drug-like potential of the known oxidized metabolites of some antioxidants was explored in our recent review.[28] Using t-distributed stochastic neighbor embedding (t-SNE) analysis, several polyphenols (resveratrol, caffeic acid and its methyl ester) were investigated alongside their

oxidized derivatives as well as approved drugs with molecular weight below 700 Daltons. The analysis revelated that while the parent compounds (resveratrol, caffeic acid and its methyl ester) were found in the same cluster, their oxidized derivatives were found in several other clusters located distantly from the parent compounds.[28] For example, a cysteine-coupled derivative of caffeic acid was identified as a chemically represented independent singleton in a cluster with Benserazide (DOPA decarboxylase inhibitor),[33] while the quinone derivatives of caffeic acid and methyl caffeate were identified as small groups, and their cluster group included Diroximel fumarate (immunosuppressant),[34] and Physostigmine (reversible cholinesterase inhibitor).[35] The distribution of these oxidized derivatives in various clusters, both near and far apart from the parent compounds, underscore the potential of these oxidized metabolites to expand chemical space in a manner relevant to drug discovery.

## 1.5 Resveratrol

### 1.5.1 Chemistry and occurrence

Resveratrol (*trans*-3,4′,5-trihydroxystilbene), which consists of two aromatic rings linked by an ethylene bridge, is one of the most popular and widely studied dietary polyphenol found in nature. It occurs in plants as *trans*-resveratrol and *cis*-resveratrol, with the *trans* form being the more biologically stable and active isomer due to its lower susceptibility to photoisomerization and oxidative degradation.[36] Additionally, resveratrol exists in glycosylated forms, primarily as *trans*-piceid and *cis*-piceid, which improve its water solubility and stability in plant tissues, allowing better storage and transport.[37] As a secondary metabolite, resveratrol is biosynthesized through the phenylpropanoid pathway, a crucial biosynthetic pathway responsible for producing flavonoids, lignin, and other polyphenolic compounds. This pathway is activated in response to environmental stressors such as pathogen attack, UV radiation, mechanical injury, and extreme temperature fluctuations, underscoring its role in plant defense mechanisms.[38] Resveratrol is naturally abundant in grapes, peanuts, pistachios, cocoa, and a variety of berries, including mulberries, blueberries, bilberries, and cranberries, with its concentration varying based on plant species, environmental conditions, and processing methods.[39] Among these sources, red grapes and their derivatives, particularly red wine, represent one of the richest dietary sources of resveratrol, a factor contributing to the well-documented "French paradox", where moderate red wine consumption is linked to cardiovascular health benefits.[40]

### 1.5.2 Pharmacokinetics and metabolism

Despite its high oral absorption rate (at least 70%), resveratrol has very poor systemic bioavailability (≈0.5%), primarily due to extensive phase I and II biotransformations in the intestinal enterocytes, the liver, and, to a lesser extent, by gut microbiota.[41] Once ingested, resveratrol is absorbed via passive diffusion and carrier-mediated transport, but its rapid metabolism into sulfated and glucuronidated conjugates limits its circulating levels and therapeutic efficacy.[42] Within enterocytes, resveratrol is metabolized by sulfotransferases (SULT1A1) and uridine 5′-diphospho-glucuronosyltransferases (UGT1A1, UGTA9), which add sulfate and glucuronide groups, respectively. These conjugated forms are actively transported out of enterocytes via BCRP and MRP2 (apical membrane) and MRP3 (basolateral membrane). A small fraction of unconjugated resveratrol enters portal circulation, but most undergo further hepatic metabolism, resulting in phase II metabolites such as resveratrol monosulfates, diglucuronides, and methylated derivatives.[41]

In the large intestine, gut microbiota reduce resveratrol to dihydroresveratrol, lunularin, and 3,4′-dihydroxy-*trans*-stilbene, extending its biological effects and altering its activity profile.[42] Studies suggest that microbial metabolism plays a crucial role in determining resveratrol bioavailability, as inter-individual variations in gut microbiota composition can influence metabolite profiles and therapeutic outcomes.[43] Resveratrol and its metabolites are excreted through urine or recycled back into the small intestine through bile, contributing to enterohepatic circulation.[41]

### 1.5.3 Pharmacological activities

Resveratrol has attracted significant attention from medicinal chemists, diet nutritionists and health professionals due to its plethora of pharmacological activities including anticancer, antioxidant, anti-inflammatory, cardioprotective, and neuroprotective effects.[38,44] These diverse biological effects stem from the ability of resveratrol to modulate multiple signaling pathways, enzymatic activities, and gene expression patterns.[45]

**Anticancer effect**: Medical literature is full of studies showing the role of resveratrol and other polyphenolic compounds in the mitigation and possible treatment of cancer. Resveratrol exerts antiproliferative, pro-apoptotic, anti-metastatic, and anti-angiogenic effects by interfering with various oncogenic signaling cascades.[46,47] Specifically, resveratrol inhibits mitogen-activated

protein kinases (MAPKs), activator protein-1 (AP-1), sirtuin-1 (SIRT1), and nuclear factor-kappa B (NF-κB), all of which play crucial roles in cancer cell survival and proliferation. Furthermore, resveratrol has been shown to arrest the cell cycle at different checkpoints, enhance apoptosis by activating pro-apoptotic proteins (p53, Bax, caspases), and suppress angiogenesis by downregulating vascular endothelial growth factor (VEGF).[48]

**Cardioprotective effect**: The cardioprotective role of resveratrol has long been reported and considered to play a key role in the 'French paradox', for its ability to reduce risk of cardiovascular disease in the French population despite a high fat diet associated with the consumption of red wines (made from grapes, which is a rich source of resveratrol).[40,49] Resveratrol exerts cardioprotective effects by reducing atherosclerosis and modulating numerous signaling pathways in the cardiovascular system, ultimately resulting in stimulating endothelial nitric oxide production, reducing oxidative stress, inhibiting vascular inflammation, and preventing platelet aggregation.[50]

**Anti-inflammatory effect**: Multiple lines of evidence from laboratory studies, both *in vivo* and *in vitro*, have shown that the anti-inflammatory properties of resveratrol are attributed to inhibiting the production of anti-inflammatory factors. Resveratrol interferes with the activation of NF-κB, a transcription factor that regulates the expression of various genes involved in inflammation such as inflammatory cytokines like tumor necrosis factor-alpha (TNF-α) and interleukin 6 (IL-6).[51] ROS accumulation resulting in oxidative stress plays a role in promoting inflammation in a wide spectrum of diseases.[52] Resveratrol exerts anti-inflammatory effects by inhibiting the production of both ROS and NO. The anti-inflammatory effect and mechanism of action of resveratrol was examined in a comprehensive review by Meng et al.[53]

**Neuroprotective effect**: Excess production of reactive oxygen species in the brain has been implicated as a common underlying risk factor for the pathogenesis of several neurodegenerative disorders, including Alzheimer's disease, Parkinson's disease, and stroke.[54] In addition to its antioxidant and anti-inflammatory activities that have provided a means to avoid neurological diseases, resveratrol inhibits beta-amyloid (Aβ) protein aggregation and modulates intracellular effectors involved in neuronal cell survival/ death. More recently, resveratrol has been proposed to exert neuroprotective effects through the activation of SIRT1, a class of deacetylase. The ability

of resveratrol to increase SIRT1 activity is also linked to deacetylation of PGC-1α.[55] Another protein affected by resveratrol, peroxisome proliferator-activated receptor-γ (PPAR-γ), has been proposed as a therapeutic target for neurodegenerative disease due to its ability to protect against mitochondrial damage.[56,57]

### 1.5.4 Resveratrol as an antioxidant

Many of the health benefits attributed to resveratrol stem from its antioxidant properties. This is greatly influenced by the redox characteristics of the phenolic hydroxyl groups and the capacity for electron delocalization within its chemical structure.[58] Resveratrol functions as an antioxidant through the following mechanisms:

- Upregulating endogenous antioxidant enzymes

Resveratrol enhances the body's intrinsic antioxidant defense by upregulating the expression and activity of key antioxidant enzymes. Notably, it increases the levels of SOD, CAT, and GPx.[44] Research indicates that resveratrol treatment leads to a significant increase in the activity of these enzymes in various cell types, and this coordinated enzymatic activity effectively reduces ROS levels, thereby bolstering the cellular antioxidant capacity.[44,53]

- Downregulating pro-oxidant enzymes

Resveratrol also exerts its antioxidant effects by suppressing the activity of pro-oxidant enzymes. Notably, resveratrol inhibits NADPH oxidase, a key enzyme complex responsible for the production of superoxide anions, thereby reducing oxidative stress at its source.[59] Additionally, resveratrol downregulates myeloperoxidase (MPO) activity, an enzyme that catalyzes the formation of hypochlorous acid from hydrogen peroxide, contributing to oxidative tissue damage.[60]

- Activation of SIRT1 and modulation of signaling pathways

Resveratrol activates SIRT1, a $NAD^+$-dependent deacetylase that plays a central role in cellular stress resistance and longevity. This activation leads to the deacetylation and activation of peroxisome proliferator-activated receptor gamma coactivator 1-alpha (PGC-1α), enhancing mitochondrial biogenesis and oxidative metabolism, which collectively reduce oxidative stress.[61]

Additionally, SIRT1 activation by resveratrol inhibits the nuclear factor kappa-light-chain-enhancer of activated B cells (NF-κB) signaling pathway, leading to decreased expression of pro-inflammatory genes and further reduction of oxidative stress.[62,63]

- Modulation of the Nrf2 pathway

Resveratrol activates the nuclear factor erythroid 2–related factor 2 (Nrf2) pathway, a critical regulator of antioxidant defense. Under oxidative stress, Nrf2 dissociates from its inhibitor, Keap1, translocates to the nucleus, and binds to antioxidant response elements (ARE) in the DNA, promoting the transcription of antioxidant genes.[64] Resveratrol facilitates this process, enhancing the expression of genes encoding for antioxidant enzymes such as heme oxygenase-1 (HO-1), NAD(P)H quinone dehydrogenase 1 (NQO1), and glutamate-cysteine ligase.[64,65] This upregulation strengthens the cellular defense against oxidative damage and contributes to the maintenance of redox homeostasis.

- Direct Scavenging of Reactive Oxygen and Nitrogen Species (RONS)

Despite the multifaceted indirect mechanisms through which resveratrol exerts antioxidant effects, it can also directly neutralize RONS due to its distinctive chemical structure. Resveratrol contains three hydroxyl groups located at positions 3,5, and 4′, along with conjugated double bonds and aromatic rings, enabling it to effectively scavenge a wide range of RONS, including superoxide anion radicals ($O_2^{\bullet-}$), hydroxyl radicals (•OH), and peroxynitrite ($ONOO^-$).[66] These hydroxyl groups allow resveratrol to donate hydrogen atoms, stabilizing free radicals and preventing oxidative damage to critical cellular components such as lipids, proteins, and DNA.[44] Moreover, the phenolic structure also facilitates chelation of redox-active metal ions like $Fe^{2+}$,[67] which further inhibits ROS generation by disrupting metal-catalyzed oxidative reactions.[66,68]

## 2.0 AIMS AND OBJECTIVES.

Considering that only marginal attention has been paid to the structural changes related to RONS scavenging carried out by antioxidants and to the related pharmacological consequences, this represents an unexplored segment of the chemical space with significant potential as a treasury of bioactive molecules. Resveratrol, one of the most popular dietary polyphenols, is renowned for its extensive pharmacological activities that have been linked to its antioxidant function. Beyond modulating pro-oxidant and antioxidant enzyme systems, resveratrol can also directly scavenge

free radicals due to its chemical structure, resulting in a wide array of oxidized metabolites expectably with modulated pharmacological activities. In this context, the primary aim of this Ph.D. study was to employ performance-based diversity-oriented synthesis to study the scavengeome of resveratrol subjected to various oxidative transformations, and to investigate the pharmacological activity of the oxidized metabolites. Thus, the following objectives were set up for this Ph.D. work;

1. **Preparation of oxidized resveratrol metabolite mixtures.** To achieve this, we aimed to cover the scavengeome of resveratrol using optimized experimental oxidation conditions for each biomimetic and biorelevant oxidant.
2. **Identification of metabolites from these oxidized mixtures**. To identify the plethora of oxidized metabolites formed, we aimed to utilize several chromatographic and metabolite profiling techniques to determine the nature of metabolites formed.
3. **Biological evaluation of oxidized mixtures**. We aimed to evaluate the pharmacological activities of the oxidized mixtures as potential inhibitors of several enzymes: angiotensin-converting enzyme (ACE), 15-lipoxygenase (15-LOX) and xanthine oxidase (XO).
4. **Chemical and biological evaluation of isolated compounds**. We aimed to isolate compounds from diverse and bioactive mixtures, identify these oxidized derivatives, and evaluate their biological activities as inhibitors of several enzymes: angiotensin-converting enzyme (ACE), 15-lipoxygenase (15-LOX), cyclooxygenase-1 and -2 (COX-1 and COX-2) and xanthine oxidase (XO). DPPH scavenging activity and the Oxygen Radical Absorbance Capacity (ORAC) of the oxidized mixtures were also aimed to be evaluated. Lastly, we aimed to develop and apply in silico methodologies in predicting the pharmacokinetic profiles and therapeutic potential.

## 3.0 MATERIALS AND METHODS

### 3.1 General information

Resveratrol (>98% pure, as determined by HPLC analysis) was purchased from Career Henan Chemical Co. (Henan province, China). Analytical grade reagents, organic solvents and HPLC solvents were purchased from Sigma (Merck KGaA, Darmstadt, Germany), Reanal Laboratory Chemicals (Budapest, Hungary) and ChemLab (Zedelgem, Belgium).

Chromatographic instruments and functional units used during this Ph.D. work include:

- HPLC (Jasco Co., Tokyo, Japan) for analytical purposes – dual PU-2080 pumps; AS-2055 Plus autosampler; MD-2010 Plus PDA detector, used with columns; Kinetex XB-C18 and Biphenyl (250 × 4.6 mm, 5 μm).
- HPLC (Agilent Technologies, Waldbronn, Germany) for semi-preparative purposes-Agilent 1100 Series system pump attached with a Jasco "UV- 2070 Plus" single-wavelength UV detector., using Gemini-NX C18 or Phenyl-hexyl column (250 x 10.0 mm, 5μm).
- HPLC (Gilson, Middleton, WI, USA) for preparative purposes - Armen Spot Prep II integrated HPLC purification system using a Kinetex XB-C18 100 Å or Biphenyl column (250 x 21.2 mm, 5μm).
- Flash chromatograph (Teledyne ISCO, Lincoln, NE, USA) for preparative purposes - Combiflash Rf+ instrument equipped with diode array and evaporative light scattering detection (DAD-ELSD) using commercially available prefilled "RediSep" columns.
- HPLC (Jasco Co., Tokyo, Japan) used for chiral separation – PU-4386 pump and PU-4086 pump; column oven (CO-4060); AS-4350 autosampler; MD-4015 PDA detector, equipped with a fraction collector.

### 3.2 Exploration of oxidized resveratrol metabolite mixtures in 96-well microplates

Each well containing 2 mM resveratrol was subjected to various oxidants/co-oxidants at varying concentrations in a 1 mL microplate (VWR Deep Well Plates, 96 Round Well European Cat. No. 732-3322) or 500 μL microplate (Grenier 786201 PP-Masterblock, 96 Well, V-Shape). ACE inhibitory screening of the oxidized mixtures was determined at the start of each reaction by transferring 5 μL aliquots of the oxidized mixture from the reaction plate to a 96-well black plate (655096, F-bottom, Grenier bio-one). Concurrently, the metabolite profile of each mixture was also determined at the start using laser-assisted rapid evaporative ionization mass spectrometry

(LA-REIMS). Subsequent bioactivity screening and metabolite profiling was conducted at specific time intervals after stopping each reaction by either by transferring a 5 µL aliquot from the reaction microplate to bioactivity microplates or adding aq. GSH solution to the respective wells (and thereafter taking 5 µL aliquot from the stopped reaction mixture).

### 3.2.1 Oxidation of resveratrol in 96-well microplates

**Reaction of resveratrol with PIFA in acetonitrile**

Resveratrol (228.28 µg/150 µL in acetonitrile) was oxidized by 350 µL acetonitrile-water solution (250 µL acetonitrile + 100 µL water) of PIFA (1, 2, 4, and 8 mM) at room temperature. ACE inhibitory activity was determined at 0 h, 2 h and 6 h, while LA-REIMS analysis was performed 0, 2, 4, and 6 h for LA-REIMS analysis. Aqueous GSH solution (614.66 µg/100 µL $H_2O$) was added to respective wells when required to stop the reaction.

**Reaction of resveratrol with AAPH and $NaIO_4$**

Resveratrol (319.52 µg/225 µL in acetonitrile) was oxidized by 250 µL aqueous solution of AAPH and 225 µL acetonitrile-water solution of $NaIO_4$ (AAPH: 2, 4, and 8 mM; $NaIO_4$: 2, 4, and 8 mM) at 65°C. After the analyses at the start of the reaction, further ACE inhibitory screening and LA-REIMS analysis was done at specific time intervals (4 h and 21 h 30 min for ACE inhibitory bioactivity; 4 h, 21 h 30 min, and 24 h for LA-REIMS analysis). Aqueous GSH solution (614.66 µg/150 µL $H_2O$) was added to the corresponding wells to stop the reaction.

**Reaction of resveratrol with PIDA in acetonitrile**

Resveratrol (228.28 µg/100 µL in acetonitrile) was oxidized by 400 µL acetonitrile-water solution (150 µL acetonitrile + 250 µL water) of PIDA (1, 2, 4, and 8 mM) at room temperature. ACE inhibitory screening was conducted at 0, 1, and 3 h, and LA-REIMS analysis at 0, 1, 2, and 3 h. The reaction was stopped with an aqueous GSH solution (461 µg/100 µL $H_2O$).

**Reaction of resveratrol with PIFA in ethanol**

Resveratrol (228.28 µg/100 µL in ethanol) was oxidized by PIFA (1, 2, 4 and 8 mM), each in 400 µL ethanol solution and the mixture stirred at room temperature. After the analyses at the start, further ACE inhibitory screening and LA-REIMS analysis was done at 30 min and 60 min, while

the LA-REIMS analysis was carried out at 30 min, 60 min and 90 min. Aqueous GSH solution (614.66 µg/100 µL $H_2O$) was added to GSH-terminated wells when required.

**Reaction of resveratrol with oxone and $H_5IO_6$ in ethanol**

Resveratrol (456.56 µg/ 225 µL in ethanol) was oxidized by 125 µL aqueous solution of oxone at (10, 20, and 40 µM) and 150 µL ethanol solution of $H_5IO_6$ ($H_5IO_6$: 1, 2, and 4 mM) at room temperature. Further ACE inhibitory activity was measured at 2 h and 6 h, with LA-REIMS analysis at 2 h, 4 h and 6 h after stopping the reaction in the corresponding wells by adding aqueous GSH solution (1.23 mg/100 µL $H_2O$).

**Reaction of resveratrol with $FeCl_3$ and $H_5IO_6$ in acetonitrile**

Resveratrol (456.56 µg/150 µL in acetonitrile) was oxidized by a 300 µL aqueous solution of $FeCl_3$ and a 550 µL acetonitrile-water solution (100 µL ACN + 450 µL H2O) of $H_5IO_6$ ($FeCl_3$: 90, 120, and 180 µM; $H_5IO_6$: 1, 2, and 4 mM) at room temperature. After analyses at the start of the reaction, further ACE inhibition screening was performed at 4 h and 20 h, with LA-REIMS analysis was carried out at 4h, 20 h, and 22 h 30 min, after adding aqueous GSH solution (1.23 mg/200 µL $H_2O$) to stop reaction in the respective wells.

**Reaction of resveratrol with $FeCl_3$ and $H_5IO_6$ in ethanol**

Resveratrol (456.56 µg/300 µL in ethanol) was oxidized by 300 µL aqueous solution of $FeCl_3$ and 300 µL ethanol solution of $H_5IO_6$ ($FeCl_3$: 10, 20, and 40 µM; $H_5IO_6$: 1, 2, and 4 mM) at room temperature. The reaction was stopped in the respective wells by adding an aqueous GSH solution in (1.23 mg /200 µL $H_2O$), and ACE inhibitory screening and LA-REIMS analysis was determined at the beginning of the reaction and at predefined time intervals (3 h and 20 h for the ACE inhibitory bioactivity; 3h, 17 h and 20 h for the LA-REIMS analysis).).

**Reaction of resveratrol with AIBN in acetonitrile**

Resveratrol (2 mM) in 150 µL in acetonitrile-water solution ($CH_3CN$:$H_2O$, 1:1) was oxidized by 350 µL aqueous solution of AIBN (15, 30, 60, and 120 mM) at 37°C. The ACE inhibitory screening and LA-REIMS analysis was determined at the start of the reaction and specific time intervals (3 h and 6 h 30 min for ACE inhibitory bioactivity; 3 h, 4 h 30 min, and 6h 30 min for

LA-REIMS analysis), after stopping the reaction by adding aqueous GSH solution (614.66 µg/100 µL $H_2O$) to the respective wells.

**Reaction of resveratrol with peroxynitrite in acetonitrile**

Peroxynitrite was prepared as described by Fasi et al,[69] with the concentration of the prepared peroxynitrite determined at 302 nm using 1670 $M^{-1}cm^{-1}$ as molar extinction coefficient.[70] Resveratrol (228.28 µg/250 µL in acetonitrile) was oxidized by 250 µL peroxynitrite solution (0.05, 0.1, 0.2, and 0.5 mM) at room temperature. The ACE inhibitory activity and LA-REIMS analysis was done at the start of the reaction. At 10 min, the reaction in corresponding wells was stopped by adding drops of diluted HCl until pH 2, with bioactivity screening and metabolite profiling subsequently done.

**Reaction of resveratrol with $NaNO_2$ in phosphate buffer, pH 3.0**

Resveratrol (2 mM, 5 µL resveratrol solution in acetonitrile) was oxidized by 495 µL phosphate-buffered solution (pH 3.0) containing $NaNO_2$ at varying concentrations (4, 8, 16, and 20 mM) at 37°C. After ACE inhibitory and LA-REIMS analyses at the start, further analysis done at 30 min and 60 min, after stopping the reaction in corresponding wells by the addition of aqueous GSH solution (614.66 µg/100 µL $H_2O$).

**Reaction of resveratrol with $NaNO_2$ in KCl-HCl, pH 2.0**

Corresponding amounts of $NaNO_2$ were dissolved in solutions of 50 mM KCl-HCl to get varying concentrations (1, 2, 4 and 6 mM) of the oxidant solution. Thereafter, 2 mM resveratrol solution (250 µg resveratrol/250 µL acetonitrile solution) was oxidized by 250 µL of each oxidant solution, and the mixture stirred at 37°C. ACE inhibitory and LA-REIMS analyses were performed at the start of the reaction and at specific time intervals (1 h and 2 h), after adding aqueous GSH solution (614.66 µg/100 µL $H_2O$) to respective wells.

**Reaction of resveratrol with AAPH and $H_2O_2$ in acetonitrile**

Resveratrol (319.52 µg/300 µL in acetonitrile) was oxidized by 250 µL aqueous solution of AAPH and 150 µL $H_2O_2$ solution (AAPH: 2, 4, and 8 mM; $H_2O_2$: 100, 200, and 400 mM) at 65°C. The reaction was stopped with aqueous GSH solution (614.66 µg/150 µL $H_2O$) in corresponding

wells, with ACE inhibitory screening and LA-REIMS analysis determined at the start of the reaction and at specific time intervals (4 h and 21 h 30 min for ACE inhibitory screening; 4 h, 21 h 30 min, and 24 h for LA-REIMS analysis.

**Reaction of resveratrol with $K_3[Fe(CN)_6]$ and $Na_2CO_3$ in acetonitrile**

Resveratrol (456.56 µg/400 µL in acetonitrile) was oxidized by 300 µL aqueous solution of $K_3[Fe(CN)_6]$ and 300 µL aqueous solution of $Na_2CO_3$ ($K_3[Fe(CN)_6$: 1, 2, and 4 mM; $Na_2CO_3$: 1, 2, and 4 mM) at room temperature. In addition to analysis at the start of the reaction, ACE inhibitory screening was done at 2 h 30 min and 20 h while LA-REIMS analysis was performed at 2 h 30 min, 17 h 30 min, and 20 h. Aqueous GSH solution (614.66 µg/200 µL $H_2O$) was added to respective wells, before analyses were carried out.

**Reaction of resveratrol with $CuSO_4$ in acetonitrile**

Resveratrol (228.28 µg/200 µL acetonitrile + 50 µL water) was oxidized by 250 µL aqueous solution of $CuSO_4$ at varying concentrations (1, 2, 4, and 8 mM) at 37°C. The ACE inhibitory screening and LA-REIMS analysis was determined at the start of the and at specific time intervals (6 h and 25 h for ACE inhibitory bioactivity; 6 h, 22 h, and 25 h for LA-REIMS analysis), after adding aqueous GSH solution (614.66 µg/100 µL $H_2O$) to respective wells.

**Reaction of resveratrol with $H_2O_2$ and 5,10,15,20-Tetrakis(pentafluorophenyl)-21H,23H-porphyrin iron(III) chloride ($C_{44}H_8ClF_{20}FeN_4$) in acetonitrile-methanol (TPF)**

Resveratrol (228.28 µg/150 µL in acetonitrile) was oxidized by 360 µL acetonitrile-methanol solution (6.2 – 1, $CH_3CN$ – $CH_3OH$) of TPF and 50 µL aqueous $H_2O_2$ solution at varying concentrations (TPF: 1, 2, and 4 mM; $H_2O_2$: 75, 150, and 300 mM) at room temperature. At the start of the reaction and at specific time intervals (1 h for ACE inhibitory bioactivity; 30 min, and 1 h), ACE inhibitory screening and LA-REIMS analysis was determined. Analyses were performed after adding aqueous GSH solution (614.66 mg/50 µL $H_2O$) to respective wells.

### 3.2.2 Metabolite fingerprinting of microplate oxidized mixtures by LA-REIMS

Metabolite profiling of the oxidized resveratrol mixtures in the microplates was studied in collaboration with the group of Prof. György Tibor Balogh of the Department of Pharmaceutical

Chemistry, Semmelweis University, Budapest, Hungary. The detailed description of the setup was published,[71]; it involved the direct analysis of the aerosolized oxidation reaction solutions using laser ablation (OPOTEK OPO laser, λ=2940nm, 5mJ/pulse, 20Hz shot frequency, 6ns pulse width) coupled with rapid evaporative ionization mass spectrometry (REIMS). In brief, after introducing the sample into the REIMS interface, ionization occurred via collision with a high-temperature impactor surface. Mass spectrometry was conducted on a Xevo G2-XS QToF spectrometer in positive and negative modes Leucine enkephalin was used as a lock mass standard, ensuring <3 ppm mass accuracy. Data processing was performed using Waters MassLynx™ 4.2 and Abstract Model Builder (AMX) software, with calibration using 0.5 mM sodium formate solution. Samples had at least two laser burns for real-time metabolite identification. Each sample had at least two laser burns (±3 seconds per burn), allowing high-throughput screening and identification of oxidized resveratrol metabolites in real-time.

### 3.2.3 ACE inhibitory screening of microplate oxidized mixtures

ACE inhibitor screening of the oxidized mixtures was measured by fluorometric assay following the method described by Sentandreu and Toldrá [72] with some modifications. Buffer A (150 mM Tris-base buffer with 1 μM $ZnCl_2$, pH 8.3) required for ACE preparation, and buffer B (150 mM Tris-base buffer with 1.125 M NaCl, pH 8.3) required for substrate buffer solutions were prepared as outlined.[73] To determine the inhibitory activity of the oxidized mixtures, to 5 μL aliquot of each mixture in a 96-well black microplate was added 15 μL buffer A, and subsequently 20 μL ACE solution (2 mU enzyme activity). After pre-incubating at 37°C for 10 minutes, 80 μL of 0.45 mM buffered substrate solution was added, and fluorescence monitored at λex/λem = 340/450 nm every minute at 37°C for 30 min using a FluoStarOptima plate reader (BMG Labtech, Ortenberg, Germany). Control samples, representing 100% enzyme activity, were prepared by substituting the mixture solution with buffer A. The percentage inhibition by each compound was calculated as; % inhibition = (control values – sample values)/(control samples) x 100

## 3.3 General procedures for resveratrol oxidation and isolation of compounds [I, II] [70,74]

Following microplate-based oxidative transformations, optimized oxidative reactions were carried out on resveratrol as reported.[70]

### 3.3.1 Reaction of resveratrol with PIFA in acetonitrile (Ox1) [II]

Briefly, resveratrol (300 mg/150 mL in acetonitrile) was oxidized by an acetonitrile solution of 1 equiv PIFA for 5 h at room temperature. The mixture was worked up and subsequently purified to obtain **1** (3.15 mg), **2** (10.13 mg) and **3** (2.93 mg)

### 3.3.2 Reaction of resveratrol with AAPH and $NaIO_4$ (Ox2) [II]

In summary, resveratrol (500 mg/250 mL in acetonitrile) was oxidized by aq. solution of 1.5 equiv AAPH and an acetonitrile solution of 1 equiv $NaIO_4$ for 23 h at 65°C, with the reaction stopped by adding aq. solution of 1.76 equiv reduced glutathione. Compounds **4** (3.24 mg), **5** (12.93 mg), **6** (11.38 mg) and **7** (2.65 mg) were isolated from this mixture.

### 3.3.3 Reaction of resveratrol with PIDA in acetonitrile (Ox3) [II]

Briefly, resveratrol (100 mg/25 mL in acetonitrile) was oxidized by an acetonitrile solution of 2 equiv PIDA for 2 h at room temperature. The reaction was stopped by adding aq. solution of 2 equiv GSH, worked up, and the resulting residue purified to get **6** (6.37 mg). Compound **6** racemate (5 mg) was separated into its enantiomers by chiral HPLC using an isocratic elution of hexane – EtOH (82:18, v/v) on cellulose tris(3,5–dimethylphenylcarbamate) coated on silica gel (Chiralcel OD-H; 250 x 4.6 mm, 5 µm, Daicel, Japan) to obtain pure enantiomers **6a** (1.89 mg) and **6b** (1.97 mg).

### 3.3.4 Reaction of resveratrol with PIFA in ethanol (Ox4) [II]

To summarize, resveratrol (250 mg/50 mL in ethanol) was oxidized by an ethanol solution of 1 equiv PIFA for 90 min at room temperature, stopped by adding an aq. solution of 2 equiv GSH, worked up and purified to obtain compounds **8** (11.93 mg), **9** (8.38 mg) and **10** (22.62 mg).

### 3.3.5 Reaction of resveratrol with Oxone and periodic acid in ethanol (Ox5) [II]

Briefly, resveratrol (600 mg/300 mL in ethanol) was oxidized by an ethanol solution of 0.005 equiv oxone and ethanol solution of 0.66 equiv $H_5IO_6$ for 7 h at room temperature. The reaction was stopped by adding an aqueous solution of 2 equiv GSH, worked up and purified to get **11** (12.41 mg), **8** (18.66 mg), **5** (167.30 mg), **12** (18.30 mg), **13** (25.94 mg), **14** (2.70 mg) and **15** (20.09 mg).

### 3.3.6 Reaction of resveratrol with $FeCl_3$ and $H_5IO_6$ in acetonitrile (Ox6) [II]

Briefly, resveratrol (480 mg/240 mL in acetonitrile) was oxidized by an acetonitrile solution of 0.03 equiv $FeCl_3$ and an acetonitrile solution of 0.8 equiv $H_5IO_6$ for 17 h at room temperature. The reaction was stopped by adding an aq. solution of 2 equiv GSH, worked up and purified to obtain compounds **16** (12.01 mg), **5** (9.13 mg) and **12** (22.27 mg).

### 3.3.7 Reaction of resveratrol with $FeCl_3$ and $H_5IO_6$ in ethanol (Ox7) [II]

Briefly, resveratrol (360 mg/180 mL in ethanol) was oxidized by an ethanol solution of 0.03 equiv $FeCl_3$ and an ethanol solution of 1.1 equiv $H_5IO_6$ for 17 h at room temperature, with the reaction stopped by adding an aq. solution of 2 equiv GSH, worked up and purified to get **5** (3.11 mg), **13** (7.67 mg), **14** (6.15 mg) and **17** (6.05 mg).

### 3.3.8 Reaction of resveratrol with AIBN in acetonitrile (Ox8) [II]

In summary, resveratrol (160 mg/7 mL, 1-6, v/v in DMSO-acetonitrile) and 20 mL ethyl linoleate (L1751, Sigma Aldrich) was oxidized by an acetonitrile solution of 31.2 equiv AIBN for 8 h at 40°C. The resulting mixture was worked up and purified to obtain a pure compound, **6** (3.19 mg).

### 3.3.9 Reaction of resveratrol with peroxynitrite in acetonitrile (Ox9) [II]

Briefly, resveratrol (114.13 mg/50 mL in acetonitrile) was oxidized by 50 mL, 0.1 mM peroxynitrite for 5 min at room temperature. The reaction was stopped by adding drops of diluted HCl until pH 2, worked up and subsequently purified to obtain compounds **2** (17.00 mg), **6** (22.63 mg) and **19** (18.61 mg).

### 3.3.10 Reaction of resveratrol with $NaNO_2$ in phosphate buffer, pH 3.0 (Ox10) [II]

To summarize, resveratrol (85.5 mg/15 mL in acetonitrile) was oxidized by phosphate-buffered sodium nitrite solution (207 mg in 1485 mL) for 1 hour at 37°C, with the reaction stopped by adding an aq. solution of 2 equiv GSH, worked up and purified to obtain compounds **4** (4.15 mg), **18** (13.03 mg) and **19** (2.84 mg).

### 3.3.11 Reaction of resveratrol with $NaNO_2$ in KCl-HCl, pH 2.0 (Ox11) [II]

Briefly, resveratrol (11.84 mg/400 mL in acetonitrile) was oxidized by a 50 mM KCl-HCl solution of 1 equiv $NaNO_2$ for 2 h at 37°C. The reaction was stopped by adding an aqueous solution of 0.8 equiv GSH, worked up and analyzed by HPLC.

### 3.3.12 Reaction of resveratrol with AAPH and $H_2O_2$ in acetonitrile (Ox12) [II]

Briefly, resveratrol (10 mg/ 6 mL acetonitrile) was oxidized by an aqueous solution of 1.5 equiv AAPH and 50 mM hydrogen peroxide for 26 h at 65°C. The reaction was stopped by adding an aqueous solution of 2 equiv GSH and worked up to give a dry residue required for HPLC analysis.

### 3.3.13 Reaction of resveratrol with $K_3[Fe(CN)_6]$ and $Na_2CO_3$ in acetonitrile (Ox13) [II]

Briefly, resveratrol (11.4 mg/4 mL in acetonitrile) was oxidized by an aqueous solution of 1 equiv potassium ferricyanide and an aqueous solution of 1 equiv sodium carbonate for 43 h at room temperature. The reaction was stopped by adding an aqueous solution of 1 equiv GSH and worked up to give a dry residue required for HPLC analysis.

### 3.3.14 Reaction of resveratrol with $CuSO_4$ in acetonitrile (Ox14) [II]

In summary, resveratrol (10 mg/10 mL; 9-1in acetonitrile-water) was oxidized by an aqueous solution of 2 equiv $CuSO_4$ for 72 h at 37°C. The reaction was stopped by adding an aqueous solution of 2 equiv GSH and worked up to give a dry residue required for HPLC analysis.

### 3.3.15 Reaction of resveratrol with xanthine oxidase in phosphate buffer, pH 7.4 (Ox15) [II]

Briefly, resveratrol (10.25 mg/5 mL DMSO) was oxidized by 0.15 mM phosphate-buffered xanthine solution and xanthine oxidase solution for 5 min at 37°C. The reaction was cooled and worked up to obtain dry residue required for HPLC analysis.

### 3.3.16 Reaction of resveratrol with $H_2O_2$ and 5,10,15,20-Tetrakis(pentafluorophenyl)-21H,23H-porphyrin Iron (III) Chloride ($C_{44}H_8ClF_{20}FeN_4$) (Ox16) [II]

Briefly, resveratrol (11.48 mg/9 mL in acetonitrile) was oxidized by a methanol-water solution of 0.2 equiv of the porphyrin iron (III) chloride and 160 mM hydrogen peroxide for 50 min at room

temperature. The reaction was stopped by adding an aqueous solution of 2 equiv GSH, worked up and purified to give a dry residue required for HPLC analysis.

### 3.4 Metabolite profile analysis [II]

In collaboration with Prof. Emerson F. Queiroz and Prof. Jean-Luc Wolfender, and their research group at the Institute of Pharmaceutical Sciences of Western Switzerland, University of Geneva, Geneva, Switzerland, the metabolite profile of the oxidized mixtures and pure compounds isolated from these mixtures were done using UHPLC-PDA-ELSD-MS and UHPLC-PDA-CAD-HRMS respectively according to previously described methods on the same instrument and under the same conditions as those described by Huber and coworkers.[75]

### 3.5 Structure elucidation of compounds

Structure elucidation of the isolated compounds was based on the information obtained through high-resolution mass spectrometry (HRMS) and nuclear magnetic resonance (NMR) spectroscopic studies. HRMS spectra were performed in a collaboration with Dr Róbert Berkecz (Institute of Pharmaceutical Analysis, University of Szeged, Szeged, Hungary), and were acquired on Q-Exactive Plus hybrid quadrupole-orbitrap mass spectrometer (Thermo Scientific, Waltham, MA, USA) equipped with heated electrospray ionisation (HESI-II) probe that was used in positive or negative mode per required. Analysis of $^{1}$H NMR, $^{13}$C, APT, HSQC, HMBC, $^{1}$H,$^{1}$H-COSY and NOESY were conducted in acetone-$d_6$ at room temperature on a Bruker DRX-500 spectrometer. The chemical shifts (δ) are given on the δ-scale and referenced to the solvents (acetone-$d_6$: δH = 2.05 and δC = 29.9 ppm); coupling constant (*J*) values are expressed in Hz. Data interpretation and spectral analysis were carried out using widely accepted strategies with MestReNova v6.0.2-5475 software (Mestrelab Research S.L., Santiago de Compostela, Spain). The NMR investigations were performed in research collaboration with Dr. Norbert Kúsz (University of Szeged, Institute of Pharmacognosy, Szeged, Hungary). The NMR investigations of compounds **2, 5-6, 8-10, 12** and **16** were performed in collaboration with Prof. Gábor Tóth (NMR Group, Department of Inorganic and Analytical Chemistry, Budapest University of Technology and Economics, Budapest, Hungary).

### 3.6 Absolute configuration of 6 enantiomers [II]

Using vibrational circular dichroism (VCD), molecular modeling and calculation of VCD spectra, the absolute configuration of the enantiomers of **6** (i.e., **6a** and **6b**) was determined in collaboration with Dr. Elemér Vass and Prof. Antal Csámpai at the Department of Organic Chemistry, Eötvös Loránd University, Budapest, Hungary. The absolute configuration of compound **6b** was determined by recording its VCD spectrum in DMSO-$d_6$ and comparing it with theoretical spectra calculated for the (2*S*,3*S*) enantiomer using B3LYP/6-311++G(d,p) level [76] with an IEF-PCM solvent model, based on Boltzmann-weighted sum of 64 conformers.

### 3.7 Biological evaluation of mixtures and compounds [I, II]

#### 3.7.1 Angiotensin-I Converting Enzyme (ACE) inhibitor activity [II]

ACE percentage inhibition and dose-response studies on resveratrol and isolated compounds were calculated by measuring the fluorescence in kinetic mode at Ex/Em 290/450 nm. The inhibition mechanism of the most potent compounds, **6** and **12**, was elucidated by ACE inhibitory kinetic studies with the $K_m$ and $V_{max}$ determined by Lineweaver-Burk plots. Subsequent to inhibitory kinetic studies, the inhibitory activity and dose-effect studies of the most active compounds (**6** and **12**) in both ACE domains was determined by measuring the fluorescence of the FRET-substrate (Abz-SDK(Dnp)P-OH and Abz-LFK(Dnp)-OH for the N- and C-domain, respectively) at λex/λem = 290/450 nm

Following domain-specific studies, the energy minimized structures of both enantiomers **6a-(*R,R*)** and **6b-(*S,S*)** were docked in the active sites of C-domain (PDB ID: 1O86) and N-domain (PDB ID: 2C6N) of ACE, obtained from the RCSB Protein Data Bank [77,78] using Autodock suite according to previously published method.[70,79,80] A zinc-centered grid box (X: 43.817, Y: 38.308, and Z: 46.652, covering 50 × 70 × 50 grid points of 0.375 Å spacing) was set for 1O86 (C-domain),[81] while a similar preparation was done for 2C6N (N-domain), defining a grid box (X: -28.034, Y: -24.612, and Z: -33.992, with 70 x 70 x 60 grid points and 0.375 Å spacing).[82] Docking with the Lamarckian genetic algorithm in AutoDock 4.2 involved 20 runs at the medium level ($2.5 \times 10^6$ evaluations), with the best confirmations determined based on binding energy values. The docking interactions were visualized using Biovia Discovery Studio after converting the generated PDBQT files to PDB format with OpenBabel GUI 2.4.1.[83]

### 3.7.3 15-Lipoxygenase (15-LOX) inhibitory activity [II]

The oxidized mixtures and pure compounds were tested for 15-LOX inhibition using the Cayman's lipoxygenase inhibitor screening assay kit (760700, Cayman Chemical, MI, USA), with minor modifications to the volume of concentration of linoleic acid substrate added to the wells as described in our study.

### 3.7.4 Cyclooxygenase (COX) inhibitory activity [II]

COX-1 and 2 inhibitory activities were tested based on the fluorometric method described in BioVision's COX-1 inhibitor screening kit leaflet (K548-100, BioVision, CA, USA) and the COX-2 inhibitor screening kit leaflet (K547-100, BioVision, CA, USA) respectively.

### 3.7.5 Xanthine Oxidase inhibitory activity [I]

The XO inhibitory activity of the oxidized mixtures and pure compounds, and dose–effect studies on the most bioactive compounds and resveratrol were tested by estimating the increase in uric acid formation at 290 nm, for approximately 150 s at 37°C, with allopurinol as the reference using the previously described method.[84] Enzyme kinetic studies of the bioactive compounds were also performed. Subsequent to the enzyme-kinetic studies, *in silico* docking was performed with the most potent competitive inhibitors **12** and **16**. To this, we followed our previously published approach using the 3NVY protein,[85] and the docking site was defined in a 10 Å radius around the experimental position of quercetin bound to the active site of XO.

### 3.7.6 DPPH Radical scavenging activity [I]

The DPPH free radical scavenging assay was conducted based on the method of Fukumoto et al.[86] by measuring absorbance at 550 nm for 30 min, and using a sigmoidal dose–response model of the blank corrected values was used to calculate $IC_{50}$ values of compounds.

### 3.7.7 Oxygen Radical Absorbance Capacity (ORAC) [I]

The oxygen radical absorbance capacity was determined as described by Dávalos et al.[87] by measuring the fluorescence at Ex/Em 485/520 every 90 s cycle time for 120 cycles. The antioxidant abilities, expressed as Trolox equivalents, were obtained by calculating the area under the fluorescence decay curve (AUC) and interpolating the net AUC against the Trolox standard curve.

## 4.0 RESULTS

### 4.1 Exploring the scavengeome of resveratrol

Oxidized resveratrol metabolite mixtures were prepared by subjecting resveratrol to various oxidative models, including several biomimetic and biorelevant oxidation approaches. These models included those that directly generate oxidative agents/free radicals naturally present in biological systems such as hydroxyl radicals (•OH), as well as generated by metalloporphyrin/$H_2O_2$, $Fe^{2+}$, or $Cu^{2+}$ systems along with $ONOO^-$, a potent RNS. Resveratrol was also oxidized by hypervalent iodine oxidants, PIDA and PIFA. Additionally, AIBN and AAPH, well-characterized radical initiators, were incorporated as experimentally validated models of oxidative stress. Similarly to peroxynitrite oxidation, resveratrol was oxidized by sodium nitrite under acidic phosphate buffer (pH 3.0) and KCl-HCl (pH 2.0). Chemical systems incorporating aqueous components in the oxidative reaction medium were also considered. To further enhance the physiological relevance of the experimental procedure, most reactions were terminated by adding GSH.

Oxidation reactions conducted in microplates resulted in a wide array of metabolite profiles, which were fingerprinted using LA-REIMS. Real-time monitoring of all oxidative reactions revealed a total of 105 and 154 m/z product ions in positive ($[M+H]^+$) and negative mode ($[M-H]^-$), respectively. ACE inhibitory screening assays were simultaneously conducted on the oxidized mixtures to obtain a time-course plot for ACE inhibition of the oxidized mixtures from the start of the reaction to the end. Majority of the oxidized mixtures exhibited >97% ACE inhibition at their peak biological activity, in contrast with resveratrol that demonstrated 35–50% inhibition in all conditions. The oxidation of resveratrol led to the formation of multiple oxidized metabolites with improved ability to inhibit the ACE enzyme compared to the parent compound.

### 4.2 Preparation and evaluation of oxidized resveratrol metabolites

Subsequent to performance-based diversity-oriented resveratrol oxidation, optimal experimental conditions were selected for the scale-up of each oxidative transformation. The resulting oxidized mixtures (Ox1–Ox16) were analyzed by HPLC-PDA to obtain chromatographic fingerprints, and subsequently by UHPLC-PDA-ELSD-MS to obtain a comprehensive overview of their metabolic profile. To gain preliminary insights into the formed metabolites, the metabolic profile of the mixtures was analyzed against a diverse array of resveratrol oligomers. At first glance

using Mzmine 4.3.0 software (mzio, GmbH), in accordance with previously published protocol,[88] the metabolite map of the oxidized mixtures, Ox1–Ox16, showed that oxidized metabolites ranged between 220–570 Da, having *m/z* values signifying resveratrol dimers, ethoxy-substituted derivatives and halogen-substituted derivatives.

**Table 1**. ACE, 15-LOX, and XO inhibitory activities of the oxidized mixtures in comparison with resveratrol, and the compounds isolated from each mixture. Results are expressed as mean ± SEM, n = 3, *: p <0.05 by one-way ANOVA using Dunnett's multiple comparison test to the parent compound, resveratrol. Resveratrol was tested at 90 µM, 40 µM and 100 µM for ACE, 15-LOX and XO inhibition screening respectively, and mixtures Ox1–Ox16 at corresponding concentrations of resveratrol equivalents.

| ID | ACE Inh. (%) | LOX Inh. (%) | XO Inh. (%) | Compound isolated |
|---|---|---|---|---|
| Res. | 35.9 ± 1.9 | 7.0 ± 1.0 | 49.9 ± 6.9 | - |
| Ox1 | 51.3 ± 1.2* | 45.9 ± 9.1* | 42.5 ± 3.3 | **1**–**3** |
| Ox2 | 69.9 ± 7.2* | 43.8 ± 3.3* | 37.6 ± 5.3 | **4**–**7** |
| Ox3 | 55.3 ± 3.3* | 56.8 ± 7.0* | 32.0 ± 2.1* | **6** |
| Ox4 | 66.7 ± 6.3* | 39.1 ± 4.0* | 47.1 ± 1.6 | **8**–**10** |
| Ox5 | 87.3 ± 1.6* | 42.1 ± 3.8* | 55.8 ± 1.8 | **5, 8, 11**–**15** |
| Ox6 | 87.7 ± 4.5* | 18.9 ± 4.5 | 67.8 ± 1.8* | **5, 12, 16** |
| Ox7 | 64.7 ± 3.5* | 2.9 ± 1.4 | 75.7 ± 4.9* | **5, 13, 14, 17** |
| Ox8 | 52.0 ± 7.2* | 20.5 ± 3.6 | 42.3 ± 2.9 | **6** |
| Ox9 | 94.3 ± 1.9* | 31.7 ± 3.8* | 63.3 ± 1.6 | **2, 6, 19** |
| Ox10 | 75.4 ± 3.4* | 30. 4 ± 5.6* | 46.9 ± 1.1 | **4, 18, 19** |
| Ox11 | 68.9 ± 0.9* | 17.0 ± 1.8 | 57.5 ± 1.5 | **19** |
| Ox12 | 48.2 ± 2.3 | 44.0 ± 3.8* | 10.9 ± 2.8 * | **2** |
| Ox13 | 64.8 ± 4.0* | 34.2 ± 2.5* | 29.7 ± 0.5* | **2, 6** |
| Ox14 | 86.1 ± 1.2* | 29.6 ± 5.1* | 31.9 ± 3.2* | **6** |
| Ox15 | 59.2 ± 1.7* | 12.7 ± 1.0 | 7.8 ± 0.6* | **6** |
| Ox16 | 47.6 ± 4.8 | 18.5 ± 3.8 | 2.1 ± 1.6* | **2** |

To evaluate their pharmacological potential, these chemically diverse oxidized mixtures were screened for inhibitory activity against ACE, LOX and XO, i.e., targets known to be modulated by resveratrol. The oxidation of resveratrol resulted in several metabolites with modulated ACE, LOX and XO inhibitory activity when compared to the parent compound (see **Table 1**). The combined evaluation of the metabolite diversity of these mixtures and their bioactivity served as a guide for the isolation of most bioactive metabolites. Bioactivity results, along with compounds isolated from each mixture are compiled in **Table 1**.

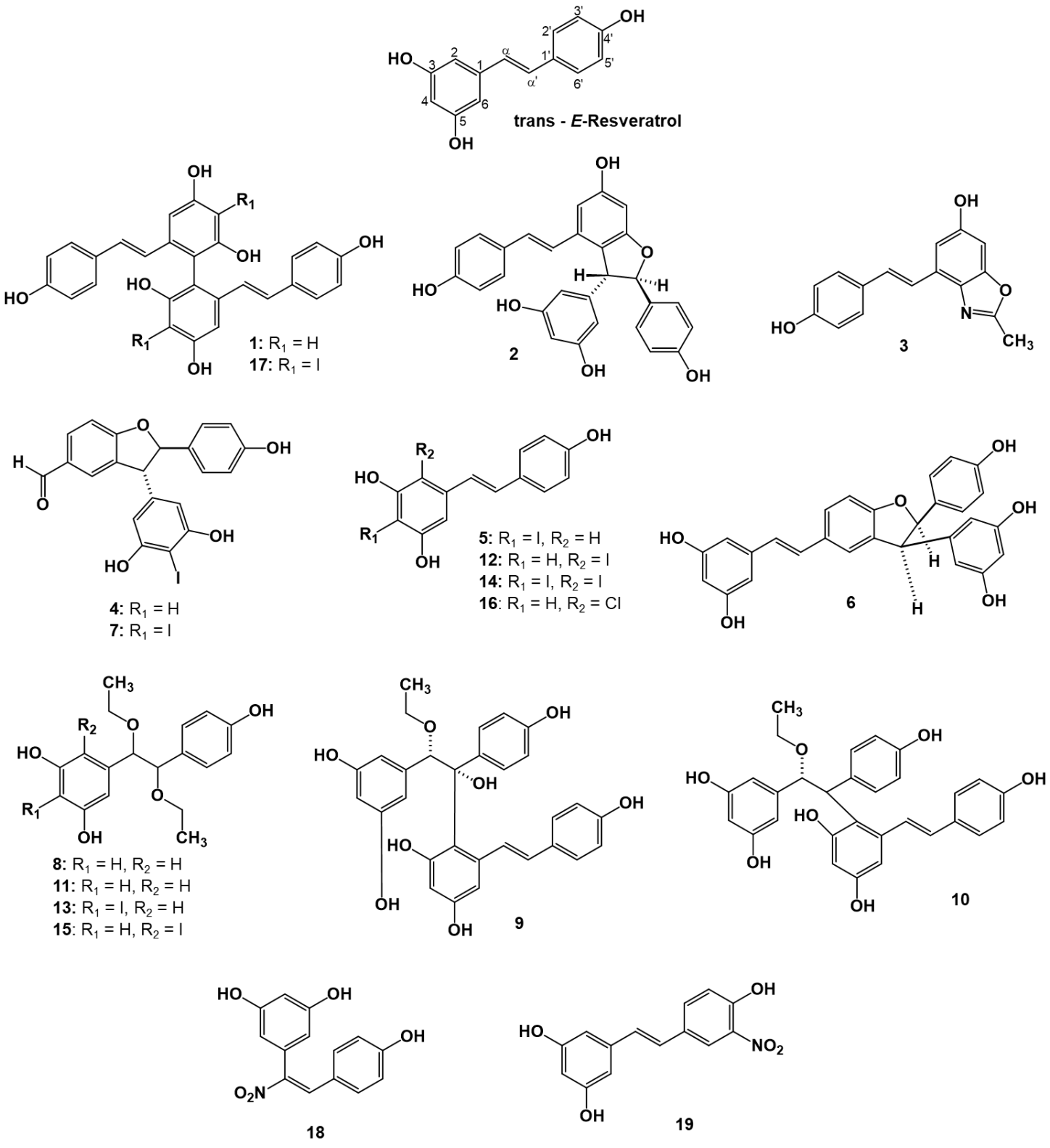


**Figure 1**: Structures of resveratrol and its metabolites obtained by chemical oxidation (**1**–**19**).

### 4.3 Structure elucidation of isolated compounds

The structures of compounds **2**, **4**, **5**, **6**, **16**, **18** and **19** were previously characterized, and, by comparing their spectroscopic information with literature values, they were identified as *trans*-ε-viniferin (**2**),[32] 3β-(3′,5′-dihydroxyphenyl)-2α-(4′′-hydroxyphenyl) dihydrobenzofuran-5-carbaldehyde (**4**),[89,90] iodo-substituted resveratrol (**5**),[91,92] *trans*-δ-viniferin (**6**),[75] chloro-substituted resveratrol (**16**),[93] and regioisomeric nitro-derivatives (**18** and **19**).[90] The structure of the other oxidized metabolites were elucidated by employing widely accepted NMR strategies,[70] and included two ethoxy-substituted dimers (**9**, **10**), two open dimers (**1**, **17**), several mono- and di-substituted iodine resveratrol derivatives (**12**, **13**, **14** and **15**) and two ethoxy-substituted monomers (**8**, **11**) as seen in **Figure 1**.

### 4.4 In silico evaluation of drug-likeness

Following the elucidation of the structure of resveratrol's oxidative metabolites, it became feasible to evaluate their drug discovery potential. The *in silico* evaluation of the compounds was done in collaboration with the group of Prof. György Tibor Balogh (Department of Pharmaceutical Chemistry, Semmelweis University, Budapest, Hungary). We employed the ACD/Percepta software package,[94] emphasizing Lipinski's rule of five (Ro5) to evaluate drug-likeness [95] and complementing it with the Ertl method to assess intestinal absorption.[96]

The principal physicochemical properties relevant to these compounds are summarized in **Table 2**, with the last column highlighting any associated medicinal chemistry rule violations (MedChem issues). In the evaluation of resveratrol and its oxidized derivatives, five compounds (**1**, **9**, **10**, **14**, **17**) exhibited violations of Lipinski's Rule of Five (Ro5), with compound **17** showing significant deviations from the optimal draggability range across three parameters. Assessment using the Ertl method indicated that compounds **1**, **10**, and **17** have a marginally reduced predicted intestinal absorption, while compound **9** is expected to have minimal absorption. Predictions of aqueous solubility categorized compounds **1**, **2**, **6**, **10**, and **14** as having moderate solubility (<0.1 mg/mL), and compound **17** as having poor solubility (<0.01 mg/mL).

Given that the ACD/Percepta software's internal database confirmed the experimentally established inhibitory impact of resveratrol on the cytochrome P450 1A2 (CyP1A2) isoenzyme, it was deemed important to evaluate this also for compounds **1**–**19**. *In silico* evaluation of the inhibitory effect of resveratrol and these compounds on the CyP1A2 isoenzyme revealed

comparable potential inhibitory effect on CYP1A2 for compounds **5**, **18**, and **19**, similar to the inhibition by resveratrol. Overall, the physicochemical characteristics of the resveratrol metabolites adhere to *in silico* drug-likeness criteria, except for compounds **1**, **9**, **10**, **14**, and **17**.

**Table 2:** Physicochemical characterization of resveratrol and its ROS/RNS-oxidized metabolites (**1**–**19**) using ACD/Percepta suite

| Compounds | MW | strongest p$K_{a,acid}$ | HBD/ HBA | log*P* / log$D_{7.4}$ | TPSA Å² | Solubility mg/ml | MedChem issues |
|---|---|---|---|---|---|---|---|
| **Resveratrol** | 228.2 | 9.2 | 3 / 3 | 2.8 / 2.8 | 60.7 | 1.23 | CyP1A2 inhibition |
| **1** | 454.5 | 8.5 | 6[#]/ 6 | 4.7[#]/ 4.7 | 121.4[#] | 0.01[#] | Ro5! (HBD) |
| **2** | 454.5 | 9.2 | 5 / 6 | 4.2 / 4.2 | 110.4 | 0.08[#] | - |
| **3** | 267.3 | 9.0 | 2 / 4 | 2.9 / 2.9 | 66.5 | 0.17 | - |
| **4** | 348.4 | 9.2 | 3 / 5 | 3.0 / 3.0 | 87.0 | 0.28 | - |
| **5** | 354.1 | 7.8 | 3 / 3 | 3.5 / 3.4 | 60.7 | 0.35 | CyP1A2 inhibition |
| **6** | 454.5 | 9.2 | 5 / 6 | 4.1 / 4.1 | 110.4 | 0.04 | - |
| **7** | 474.3 | 7.8 | 3 / 5 | 3.9 / 3.7 | 87.0 | 0.11 | - |
| **8** | 318.4 | 9.2 | 3 / 5 | 2.9 / 2.8 | 79.2 | 0.31 | - |
| **9** | 516.5[#] | 9.2 | 7[#]/ 8 | 3.9 / 3.9 | 150.8[##] | 0.19 | Ro5! (MW, HBD), TPSA! |
| **10** | 500.5[#] | 9.2 | 6[#]/ 7 | 4.5 / 4.5 | 130.6[#] | 0.02[#] | Ro5! (MW, HBD) |
| **11** | 318.4 | 9.2 | 3 / 5 | 2.9 / 2.8 | 79.2 | 0.31 | - |
| **12** | 354.1 | 8.1 | 3 / 3 | 4.1 / 4.0 | 60.7 | 0.24 | - |
| **13** | 444.3 | 7.7 | 3 / 5 | 3.8 / 3.6 | 79.2 | 0.17 | - |
| **14** | 480.0 | 6.6 | 3 / 3 | 5.1[#]/ 4.1 | 60.7 | 0.04[#] | Ro5! (log*P*) |
| **15** | 444.3 | 8.0 | 3 / 5 | 4.1 / 4.0 | 79.2 | 0.13 | - |
| **16** | 262.7 | 8.1 | 3 / 3 | 3.7 / 3.6 | 60.7 | 0.36 | - |
| **17** | 706.3[##] | 6.7 | 6[#]/ 6 | 6.8[##]/ 5.7 | 121.4[#] | 0.002[##] | Ro5! (MW, HBD, log*P*) |
| **18** | 273.2 | 8.8 | 3 / 6 | 2.5 / 2.5 | 106.5 | 0.5 | CyP1A2 inhibition |
| **19** | 273.2 | 6.8 | 3 / 6 | 3.0 / 2.3 | 106.5 | 0.5 | CyP1A2 inhibition |

[#]moderate or [##]increased violations using classical rule of five [94] or for TPSA ([#]>120 Å², [##]>140 Å²) or for Solubility ([#]<0.1 mg/ml, [##]<0.01 mg/ml).

### 4.5 Bioactivity of the oxidized metabolites

#### 4.5.1 Cardiovascular protective activity

The ACE inhibitory activity of the oxidized metabolites was evaluated and compared to that of resveratrol to assess their cardioprotective potential. Results are compiled in **Table 3**.

**Table 3.** ACE inhibitory activity and ligand-lipophilicity efficiency (LLE) of resveratrol and the isolated pure compounds. Results are expressed as mean ± SEM, n = 3 for % inhibition studies and n = 2 for $IC_{50}$ estimation. % inhibition of the compounds was performed at 90 µM and captopril at 10 µM. *: $p < 0.05$ by one-way ANOVA using Dunnett's multiple comparison test to the parent compound resveratrol. Ligand-lipophilicity efficiency values are calculated by LLE=$pIC_{50}$-logP using the log*P* values from **Table 2**.

| Compounds | ACE Inh. (%) | ACE $IC_{50}$ (µM) | LLE |
|---|---|---|---|
| Resveratrol | 38.6 ± 0.6 | **185.8** ± 9.1 | **0.9** |
| **1** | 87.4 ± 1.6 | **17.5** ± 4.8* | **0.0** |
| **2** | 81.8 ± 1.0* | **31.8** ± 0.5* | **0.3** |
| **3** | 33.4 ± 1.0 | **106.4** ± 2.0 | **1.0** |
| **4** | 66.9 ± 2.6* | **41.6** ± 2.4* | **1.4** |
| **5** | 70.9 ± 9.3* | **20.4** ± 2.2* | **1.2** |
| **6** | 101.0 ± 0.4* | **9.2** ± 0.6* | **0.9** |
| **7** | 82.0 ± 2.8* | **17.1** ± 1.8* | **0.9** |
| **8** | -7.9 ± 2.7* | **>1000** | **-** |
| **9** | 91.5 ± 0.2* | **36.5** ± 0.8* | **0.5** |
| **10** | 74.5 ± 5.3* | **33.3** ± 1.5* | **-0.1** |
| **11** | -2.9 ± 1.0* | **>1000** | **-** |
| **12** | 90.5 ± 0.7* | **15.1** ± 1.5* | **0.7** |
| **13** | 10.8 ± 2.1 | **>1000** | **-** |
| **14** | 81.8 ± 9.3* | **16.2** ± 1.7* | **-0.3** |
| **15** | 0.5 ± 3.0* | **>1000** | **-** |
| **16** | 62.4 ± 0.1 | **61.6** ± 3.4* | **0.5** |
| **17** | 71.4 ± 4.9* | **38.8** ± 1.1* | **-2.4** |
| **18** | 10.7 ± 0.3* | **277.7** ± 7.8 | **1.1** |
| **19** | 28.1 ± 2.8* | **192.4** ± 2.5 | **0.7** |
| Captopril | 81.2 ± 1.0* | **0.12** ± 0.1* | **-** |

Remarkably, most of the oxidized resveratrol derivatives obtained in this study exhibited significantly stronger ACE inhibitory compared to the moderately active resveratrol itself. Several halogenated derivatives (**5**, **7**, **12**, **14** and **17**) had markedly improved inhibitory activity. Compounds with ethoxy groups replacing the CH=CH double bond, as in **8**, **11**, **13** and **15**, had a complete loss of ACE inhibitory activity. Dimers, open- and ring-closed, had improved bioactivities, with *trans*-δ-viniferin (**6**) identified as the most potent ACE inhibitor in this study,

over 20 times stronger than resveratrol. Connecting two monomers at the CH=CH bond, such as in **9** and **10**, resulted in reduced activity compared to that of their aromatic ring-connected counterpart **1**. Additionally, fragmented dimers (**4** and **7**), which are clearly products of subsequent oxidative transformations, were also active.

Given that 11 derivatives were found to have $IC_{50}$ values less than 50 $\mu$M, we employed the LLE metric [97] to tackle and minimize the promiscuity risk in selecting ACE selective candidates. According to the method proposed by Leeson,[98] derivatives **4**, **5**, **6** and **7**, each with LLE $\geq$ 0.9 (equivalent to or larger than resveratrol) contain enthalpically more favorable binding characteristics for ACE (see **Table 3**). Altogether, based on $IC_{50}$ and LLE values, and drug-like physicochemical properties, compounds **6** and **12** were highlighted as the most promising ACE inhibitor candidates among the compounds in this study.

**Kinetic and domain specific studies of 6 and 12 as ACE inhibitors**

Enzyme kinetic studies were performed to evaluate the mode of ACE inhibition by compounds **6** and **12**. Our results revealed **6** as a competitive, and **12** as a mixed-type inhibitor.

**Table 4**: Inhibitory activity of compounds **6** and **12** on the C- and N-terminal domain of rabbit lung ACE. Results are expressed as mean ± SEM, n = 3 for % inhibition and n = 2 for dose-response studies; n. d. = not determined. For both % inhibition and dose-response studies, the substrate concentration [S] = $K_M$ was calculated from initial velocity studies of both substrates; Abz-SDK(Dnp)P-OH; [S] = 79 μM and Abz-LFK(Dnp)-OH; [S] = 33 μM.

| Inhibitor | C-domain | | N-domain | |
|---|---|---|---|---|
| | Inhibition (%)[a] | $IC_{50}$ (μM) | Inhibition (%) | $IC_{50}$ (μM) |
| **6** | 46.3 ± 4.2 | 17.1 ± 1.2 | 22.4 ± 0.7 | 56.4 ± 5.2 |
| **12** | 35.0 ± 3.3 | 35.1 ± 1.5 | 12.8 ± 1.9 | 104.8 ± 3.4 |
| BPPb | 80.9 ± 3.1 | n. d. | 0.6 ± 0.4 | n. d. |
| Angiotensin II | 36.8 ± 1.1 | n. d. | 6.1 ± 1.1 | n. d. |

[a] Inhibition percentage was determined at 10 μM for angiotensin II, and compounds **6** and **12**, and at 200 nM for BPPb.

ACE consists of two homologous metallopeptidase domains, N- and C-terminal domain (N-ACE and C-ACE, respectively).[78] Based on this, we studied the action of compounds **6** and **12** on

both domains using domain specific substrates, Abz-SDK(Dnp)P-OH (for N-ACE) and Abz-LFK(Dnp)-OH (for C-ACE). To validate the method, angiotensin II and bradykinin potentiating peptide B (BPPb), a highly specific C-ACE inhibitor, were used as positive controls. The percentage inhibition and the dose-dependent inhibition of the compounds on each domain is presented in **Table 4**. For both natural oligopeptides, BPPb and angiotensin II, the inhibition of the C-domain was significantly higher than that of the N-domain at the same inhibitor concentration, which corroborates previous studies.[99,100] Both compounds **6** and **12** also preferentially inhibited the C-domain part of the ACE. The inhibition constants of **6** bound to ACE; C-domain (Ki = 9.9 x $10^{-6}$ M) and N-domain (Ki = 2.7 x $10^{-5}$ M) showed that compound **6** preferentially inhibits the C-domain of the enzyme, with a selectivity factor of 2.74.

**Chemical and biological evaluation of *trans*-δ-viniferin enantiomers**

Chiral HPLC using an isocratic elution of *n*-hexane-ethanol (82:18, v/v) on a cellulose-based chiral column (Chiralcel OD-H) confirmed C-domain-specific ACE inhibitor *trans*-δ-viniferin (**6**) was a racemic mixture. The racemate, **6** was separated to pure enantiomers (**6a** and **6b)** in a similar workflow as previously reported by Huber and colleagues.[75] A comparison of the experimental and theoretical VCD spectra of the separated **6b** indicated that the absolute configuration of this enantiomer is (*S,S*), due to a strong correlation between the measured spectrum and the population-weighted (average) calculated spectrum.[70]

**Table 5**: ACE inhibitory activity of resveratrol and isolated enantiopure compounds. Results are expressed as mean ± SEM, n = 4 for % inhibition studies and $IC_{50}$ estimation. Inhibition % of the compounds was tested at 50 µM. *: $p < 0.05$ by unpaired t-test assuming Gaussian distribution (parametric test) between the enantiomers.

| Compound | ACE Inhibition (%) | ACE $IC_{50}$ (µM) |
|---|---|---|
| **6** | 96.3 ± 0.3 | 10.9 ± 0.1 |
| **6a**-(*R,R*) | 99.4 ± 0.5 | 8.7 ± 0.6 |
| **6b-(***S,S***)** | 91.2 ± 0.9 | 12.1 ± 0.1* |

Assessment of the ACE inhibitory activity of the *trans*-δ-viniferin enantiomers indicated a significantly higher potency of **6a-(***R,R***)** compared to its stereoisomeric counterpart, **6b-(***S,S***)** (see

**Table 5**). Following chemical and biological evaluations of these enantiomers, docking simulations were carried out to explore the interactions between both compounds with ACE at the C- and N-terminal active sites. The best docked position of both enantiomers in the ACE C-domain and N-domain active site are shown in **Figure 2**.

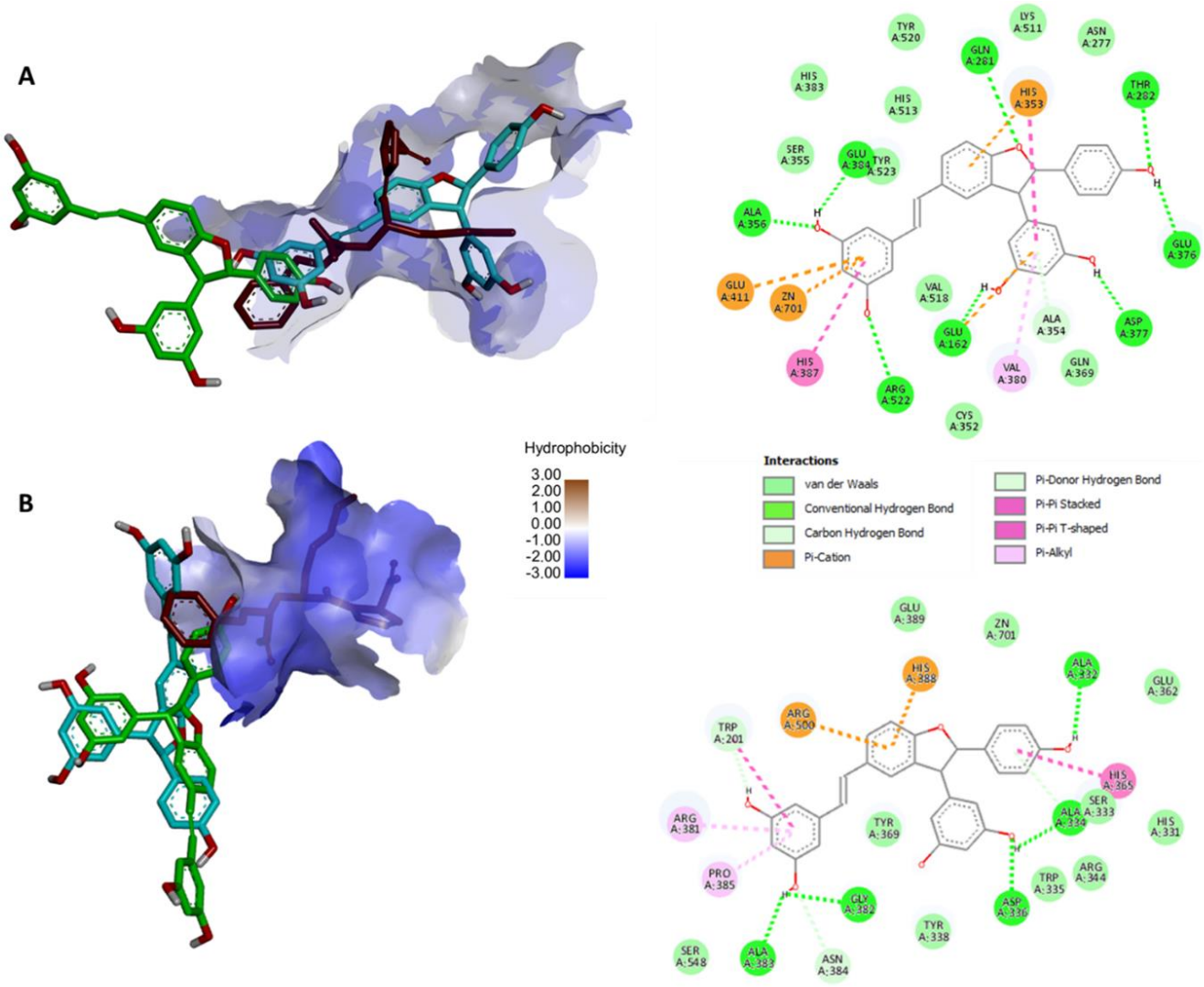


**Figure 2**. **A**: The best docked position of enantiomers **6a-(*R,R*)** in blue and **6b-(*S,S*)** in green, along with the experimental position of lisinopril (red) in the ACE C-domain active site along with the interaction map of **6a-(*R,R*). B**: The best docked position of enantiomers, **6a-(*R,R*)** in blue and **6a-(*S,S*)** in green, along with the experimental position of lisinopril (red) in the ACE active site along with the interaction map of **6b-(*S,S*)** in the A-chain of ACE N-domain.

### 4.5.2 Anti-inflammatory activities

The potential anti-inflammatory activities of the isolated compounds, relative to resveratrol, were evaluated based on their inhibitory effects on 15-LOX, COX-1 and COX-2 enzymes. Results are shown in **Table 6**.

**Table 6:** Anti-inflammatory activities of resveratrol and compounds **1**–**19**. Positive controls were SC560, Celecoxib, and NDGA for COX-1, COX-2, and 15-LOX, respectively. Results are expressed as mean ± SEM, n = 3. Compounds were tested at 100 μM for LOX % inhibition and 50 μM for COX-1 and COX-2 % inhibition. Dose-response studies were carried out on compounds exhibiting ≥ 70% and 80% inhibition for COX-1 and COX-2, respectively; n.d. = not determined. Ligand-lipophilicity efficiency values were calculated as LLE=p$IC_{50}$-log*P* using log*P* values from **Table 2**.

| **Compounds** | **COX-1** Inh.(%)/**$IC_{50}$ (μM)/LLE** | **COX-2** Inh.(%)/**$IC_{50}$ (μM)/LLE** | **LOX** Inh.(%)/**$IC_{50}$ (μM)/LLE** |
|---|---|---|---|
| **Resveratrol** | 98.6 ± 0.2/**2.9** ± 1.0/**2.7** | 95.8 ± 1.3/**5.4** ± 0.1/**2.4** | 4.3 ± 6.3/> 400 |
| **1** | 65.2 ± 5.2/ n.d. | 86.5 ± 2.8/**5.2** ± 0.3/**0.5** | 59.8 ± 7.4/**53.4** ± 5.0/**-0.5** |
| **2** | 80.0 ± 1.4/**9.1** ± 1.6/**0.9** | 91.7 ± 2.5/**3.4** ± 0.1/**1.3** | 85.8 ± 3.9/**9.7** ± 2.8/**0.8** |
| **3** | 41.5 ± 4.1/n.d. | 72.0 ± 5.2/n.d. | 35.0 ± 7.1/**85.7** ± 20.1/**1.1** |
| **4** | 37.9 ± 3.9/n.d. | 80.1 ± 2.5/**19.6** ± 1.4/**1.7** | 9.9 ± 6.9/**241.1** ± 21.0/**0.6** |
| **5** | 73.9 ± 5.3/**21.3** ± 0.7/**1.1** | 78.5 ± 2.1/n.d. | 18.7 ± 5.0/**120.6** ± 4.9/**0.4** |
| **6** | 98.6 ± 0.3/**4.7** ± 0.3/**1.2** | 92.7 ± 0.9/**5.6** ± 0.6/**1.1** | 73.1 ± 4.4/**22.4** ± 8.8/**0.5** |
| **7** | 37.1 ± 2.8/n.d. | 60.6 ± 5.7/n.d. | -14.5 ± 15.8/n.d. |
| **8** | 16.8 ± 7.9/n.d. | 38.9 ± 4.9/n.d. | -2.7 ± 4.7/n.d. |
| **9** | 29.5 ± 6.0/n.d. | 77.7 ± 2.9/n.d. | 13.5 ± 14.8/**99.6** ± 5.1/**0.1** |
| **10** | 65.9 ± 13.1/n.d. | 85.2 ± 2.0/**12.2** ± 0.2/**0.4** | -8.6 ± 7.6/n.d. |
| **11** | 17.4 ± 3.3/n.d. | 19.2 ± 6.0/n.d. | -7.4 ± 8.6/n.d. |
| **12** | 67.3 ± 2.9/n.d. | 93.2 ± 0.9/**11.1** ± 0.4/**0.8** | 19.9 ± 12.8/**97.2** ± 2.4/**-0.1** |
| **13** | 29.8 ± 16.4/n.d. | 70.2 ± 1.6/n.d. | -11.5 ± 9.0/n.d. |
| **14** | 26.5 ± 0.6/n.d. | 67.1 ± 3.6/n.d. | 20.3 ± 5.0/**97.2** ± 2.4/**-1.0** |
| **15** | 9.5 ± 1.9/n.d. | 37.9 ± 3.6/n.d. | -1.2 ± 6.8/n.d. |
| **16** | 49.1 ± 3.3/n.d. | 88.2 ± 1.1/**13.3** ± 0.1/**1.2** | 11.6 ± 4.7/**94.4** ± 3.8/**0.3** |
| **17** | 42.6 ± 17.8/n.d. | 60.6 ± 2.8/n.d. | 24.2 ± 8.1/174.9 ± 2.2/**-3.1** |
| **18** | 55.8 ± 4.0/n.d. | 48.8 ± 4.2/n.d. | 6.2 ± 1.1/>400 |
| **19** | 77.0 ± 1.1/**19.8** ± 0.1/**1.7** | 57.5 ± 4.9/n.d. | -0.48 ± 3.8/n.d. |
| Control | 100.4 ± 10.6/0.011 ± 0.1 | 77.7 ± 1.4/0.5 ± 0.1 | 80.19 ± 6.4/3.5 ± 0.8 |

*Trans*-ε-viniferin (**2**) and *trans*-δ-viniferin (**6**) had markedly improved LOX inhibitory activity corroborating previous study on the Fe-catalyzed, biomimetic oxidation of resveratrol,[32] with *trans*-ε-viniferin acting as a 40 times stronger 15-LOX inhibitor than resveratrol. Open ring dimers, **1** and **9**, also had improved activities, and several iodinated compounds (**5, 12** and **14**) exhibited pronounced LOX inhibition. Apart from the viniferins **2** and **6**, which were comparably potent, most of the oxidized derivatives obtained in this study were less effective as COX inhibitors when compared to resveratrol. Interestingly, compound **2** had a nearly 3-times selectivity towards COX-2, in contrast with resveratrol that was slightly COX-1 selective in this study.

Anti-inflammatory effects were also assessed using the ligand-lipophilicity efficiency (LLE) metric (see **Table 6**). Since the oxidized derivatives could not be proven to possess an improved inhibitory effect of COX-1 and COX-2 in comparison to resveratrol, only the relative LLE values were assessed. Thus, rating the resveratrol derivatives revealed that on COX-1 they had the enthalpically beneficial order of effect as **19** > **6** > **5** > **2**, whereas in case of COX-2, this was **4** > **2** > **16** > **6** > **12** > **1**. For LOX inhibition, only $IC_{50}$ values below 50 μM were taken into consideration, and as such, compounds **2** and **6** were identified as the two main enthalpically valuable candidates, which could potentially be considered as the order related to the LLE value.

**4.5.3 Xanthine oxidase inhibition and free radical scavenging activity.**

XO inhibitory activity of the compounds was estimated based on their ability to prevent uric acid formation from xanthine. To evaluate the potential direct antioxidant activity of the compounds in comparison with that of resveratrol, both DPPH scavenging activity and ORAC were evaluated. Results are presented in **Table 7**.

Oxidation of resveratrol resulted in the formation of some metabolites with significantly enhanced ability to inhibit XO compared to resveratrol, as shown in **Table 7**. Compounds **5**, **12**, and **16** exerted a nearly complete inhibition of XO at 100 μM, and dose–response studies revealed that **12** and **16** showed similar efficacy in XO inhibition comparable to allopurinol, a standard reference drug. Enzyme inhibition kinetics studies revealed that compounds **12** and **16** inhibit XO competitively, compound **18** and the viniferins (**2** and **6**) were observed to be mixed-type inhibitors. In silico docking was performed with **12** and **16**, the most potent competitive inhibitors, and the best-docked position of both compounds in XO active site is presented in **Figure 3**.

**Table 7**: XO inhibitory activity along with DPPH scavenging activity and ORAC values of compounds **1**–**19**. Results are expressed as mean ± SEM, n = 3 for % inhibition studies and $IC_{50}$ estimation. *: $p < 0.05$ by one-way ANOVA using Dunnett's multiple comparison test to the parent compound, resveratrol. $n = 2$ for DPPH and 3 = ORAC assay. For XO studies, $n = 4$; due to the large differences, statistical significance was not evaluated for $IC_{50}$ values.

| Compounds | XO<br>Inh.(%) / $IC_{50}$ (µM) | DPPH<br>$IC_{50}$ (µM) | ORAC<br>(Trolox Equivalent, TE) |
|---|---|---|---|
| **Resveratrol** | 55.6 ± 1.1/119.4 ± 2.0 | 27.7 ± 1.4 | 8.9 ± 0.2 |
| **1** | 30.7 ± 1.7/ n.d. | 45.59 ± 1.9 | 4.8 ± 0.3* |
| **2** | 69.1 ± 3.1/22.8 ± 6.3 | 92.1 ± 1.6 | 15.2 ± 0.5* |
| **3** | 6.5 ± 1.4*/ n.d. | 114.9 | 7.0 ± 0.2* |
| **4** | 32.9 ± 1.0/ n.d. | >500 | 8.6 ± 0.1 |
| **5** | 97.2 ± 4.9*/15.3 ± 1.4 | 41.0 ± 1.5 | 9.9 ± 0.5* |
| **6** | 77.4 ± 2.1/16.4 ± 1.3 | 340.7 ± 2.1 | 12.5 ± 0.7* |
| **7** | 23.0 ± 3.3/ n.d. | >500 | 9.2 ± 0.5 |
| **8** | 14.4 ± 3.0*/>1000 | >500 | 8.1 ± 0.5 |
| **9** | 31.5 ± 4.8/234.1 ± 4.8 | 22.6 ± 1.9 | 9.5 ± 0.3 |
| **10** | 15.1 ± 1.7*/233.3 ± 5.1 | 53.1 ± 1.5 | 13.9 ± 0.1* |
| **11** | 15.0 ± 1.4*/ n.d. | >500 | 8.1 ± 0.5 |
| **12** | 93.8 ± 1.3*/6.4 ± 0.5 | 51.7 ± 1.6 | 12.5 ± 0.7* |
| **13** | 26.5 ± 1.6/ n.d. | >500 | 11.0 ± 0.8* |
| **14** | 45.3 ± 3.0/ n.d. | 150.3 ± 1.5 | 10.5 ± 0.9 |
| **15** | 22.1 ± 0.7*/ n.d. | 233.8 ± 5.8 | 9.3 ± 0.7 |
| **16** | 90.6 ± 4.4*/4.8 ± 0.8 | 15.8 ± 1.0 | 9.9 ± 0.5 |
| **17** | 64.4 ± 0.3/ n.d. | 87.1 ± 2.9 | 8.3 ± 0.1 |
| **18** | 87.7 ± 1.8/15.7 ± 0.4 | >500 | 4.7 ± 0.1* |
| **19** | 66.6 ± 2.1/22.1 ± 0.8 | >500 | 4.5 ± 0.1* |
| **Standard** | 97.3 ± 0.9*/5.9 ± 0.9 | - | - |

A chlorine-substituted metabolite, **16**, exhibited improved DPPH scavenging activity compared to the parent compound, resveratrol. Several compounds including *trans*-ε-viniferin (**2**) and *trans*-δ-viniferin (**6**), and iodine-substituted derivatives (**12** and **13**) had significantly higher TE value than resveratrol.

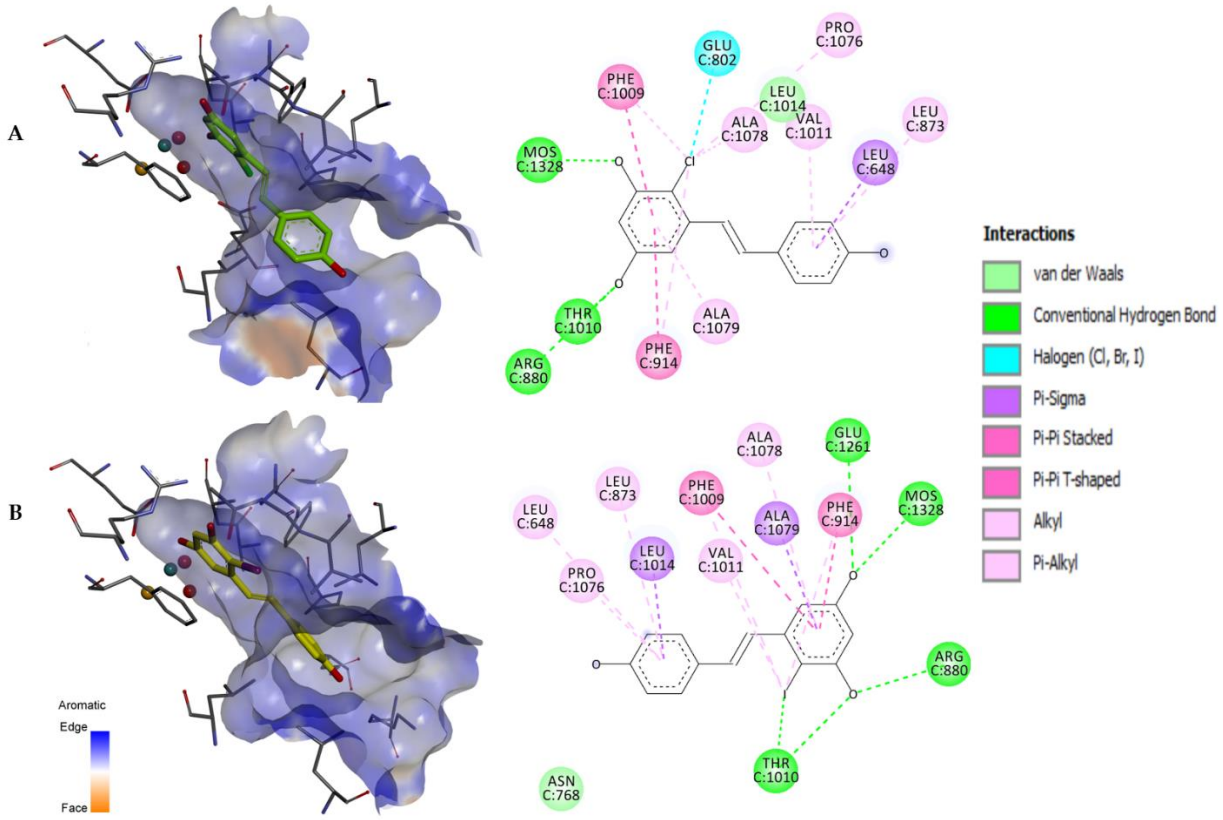


**Figure 3**. Best-docked poses of compounds **16** (**A**) and **12** (**B**). Three-dimensional orientation and aromatic edge/face receptor surface is shown for both compounds at identical viewing angle and zoom (**left**), along with the 2D interpretation of the ligand–residue interactions with the 3NVY protein (**right**).

## 5.0 DISCUSSION

### 5.1 Oxidative transformation models

In our novel approach to introduce potentially diverse oxidative chemical model systems in exploring a broad chemical space of oxidized resveratrol metabolites, we employed 'biomimetic' and 'biorelevant' models that are considered similar to human physiological processes, along with biomimetic-related chemical oxidation.[28] Accordingly, biorelevant *in vitro* models included those that directly provide free radicals that occur as such in the body, e.g., $^{\bullet}OH$. These include systems like metalloporphyrin/$H_2O_2$, $Fe^{2+}/H_2O_2$, $H_2O_2$: $Cu^{2+}$/ascorbic acid, and $ONOO^-$ as described in our previous publication.[28] Additionally, the chemical systems with substantial experimental evidence of their suitability for biological oxidative stress (DPPH, AAPH, AIBN) were also considered. For

biomimetic models, chemical systems involved an oxidation medium containing an aqueous component in addition to a cosolvent, providing a medium that may serve as a good model to the physiological conditions.[28] Chemical oxidation related to biomimetic models, differed from biomimetic only in the anhydrous organic solvent medium ($CH_3CN$, $CH_3OH$, EtOH, DMSO), which may still provide relevant models of oxidative processes within biological membranes. We therefore considered electron donors (e.g. $NaIO_4$, $K_3Fe(CN)_6$, $Cu^{2+}$, $Fe^{2+}/Fe^{3+}$) and agents that mimic the nitrating capacity of peroxynitrite (e.g. $NaNO_2$).

Synthetic metalloporphyrin models complexed with donor oxidants like $H_2O_2$ have been developed as oxidative catalysts,[101] similar to cytochrome P-450 metalloporphyrin containing proteins/enzymes. In biological systems, $H_2O_2$ generates hydroxyl radical by electron abstraction from iron or copper ions (metals abundant in biological systems), with the original metal ions regenerated by $O_2^{\bullet-}$, a two-step process that culminates in ROS generation.[13] Furthermore, AIBN and AAPH, well-characterized radical initiators that decompose to generate alkylperoxyl and alkoxyl radicals, respectively, have been utilized as experimentally validated oxidative stress models.[102,103] We also considered oxidation by hypervalent iodine (III) reagents PIFA and PIDA; these reagents were found in previous studies to reasonably mimic reactions that could occur via ROS scavenging by an antioxidant.[104,105] Additionally, xanthine oxidase was also used; it is a key enzyme in purine catabolism, and catalyzes xanthine and hypoxanthine oxidation to uric acid while generating ROS ($O_2^{\bullet-}$ and $H_2O_2$).[106] This supports its high relevance as a biochemical model for oxidative stress.

One of the most important RNS found in biological systems is peroxynitrite, formed from the reaction of the two radicals; nitric oxide (NO), an ubiquitous intracellular messenger, and $O_2^{\bullet-}$.[107] In biological environments, peroxynitrite is rapidly converted to peroxynitrous acid (ONOOH), a strong oxidizing agent.[108] Under acidic conditions, as present in the stomach, nitrite acts as an oxidizing agent,[109] justifying our studies on the transformations of resveratrol with sodium nitrite under acidic phosphate buffer (pH 3.0) and KCl-HCl (pH 2.0) as biomimetic models,[90,109] mimicking gastric oxidative conditions.

Several reactions were also performed in ethanol, to expand our work towards oxidations that may occur in aged wine bottles. As stated in our published studies,[70,74] most reactions were terminated by adding aqueous solution of reduced glutathione (GSH), an abundant intracellular antioxidant and redox buffer [110] to further improve the biorelevance of the experimental procedure.

### 5.2 The chemical space of resveratrol

Diversity-oriented synthesis to create chemical libraries for drug discovery purposes requires methodologies that are not only diverse but also have a high pharmacological hit rate,[111,112] termed biological performance diversity.[113] Our study approached this subject by exploring the chemical space of the oxidized metabolites prepared via chemical models of ROS/RNS scavenging by resveratrol. Oxidized resveratrol metabolite mixtures in microplates were screened using LA-REIMS, a powerful analytical technique for metabolite fingerprinting that enables real-time monitoring of chemical reactions and metabolic processes by ionizing molecules directly from the sample surface without extensive sample preparation. This allowed the identification of key oxidative resveratrol metabolites, offering insights into resveratrol's chemical reactivity and its scavengeome. Several m/z product ions such as dimers ($M+H^+$: 455.1478, $M-H^-$: 453.1337), ethoxy-dimers ($M+H^+$: 501.1919), iodo-substituted and chloro-substituted resveratrol moieties ($M+H^+$: 352.9670, $M+H^+$: 261.0355, respectively) and nitro-substituted derivatives ($M-H^-$: 272.0563), were easily identifiable based on literature.[74,114-116] These m/z values were observed to be common across all oxidized mixtures, with variations in peak intensity and quantity depending on oxidant concentration and reaction time in each experimental set-up. Although diversity-oriented synthesis creates large, diverse chemical libraries, there is no guarantee that the newly formed compounds have significant biological activity, causing redundancy.[113] To minimize this, the oxidized mixtures were pre-screened by their ACE inhibitory potential, allowing for the selection of conditions that result in biologically important metabolites.

Dietary antioxidants such as resveratrol may directly scavenge reactive oxygen and nitrogen species (RONS), producing a complex array of metabolites that exhibit modulated pharmacological activities when compared to their corresponding parent antioxidants.[29] The discovery of bioactive metabolites relies upon the biological assessment (screening) of collections (or libraries) of these metabolites to identify those with desired properties (hits).[117,118] A key challenge remains optimizing the balance between broad chemical space coverage and biological relevance. Although several reaction conditions resulted in a more-diverse chemical space, they did not correlate with enhanced ACE inhibitory activity. For example, some oxidized mixtures exhibited higher bioactivity at earlier time points but lacked structural diversity, as observed in resveratrol oxidation with 8 mM AAPH + 100 mM $H_2O_2$, which had an 80% inhibition at 4 h, but declined to about 45% inhibition at 21 h 30 min. Thus, we approached this challenge by prioritizing

reaction conditions favoring dimer formation ($M+H^+$: 455.1478, $M-H^-$: 453.1337), which were deemed better products for our scavengeome concept and linked to increased bioactivity.

The oxidation conditions optimized for high chemical diversity and bioactivity were scaled up to focus exclusively on significant experimental parameters. Metabolomic profiling of these optimized oxidized mixtures against a diverse array of resveratrol derivatives showed that many metabolites had *m/z* values characteristic of resveratrol dimers, in addition to ethoxy- or halogen-substituted derivatives. Resveratrol can efficiently scavenge various types of ROS/RNS, resulting in radical intermediates stabilized via electron delocalization across the two aromatic rings and the unsaturated methylene bridge connecting them.[119] Such transformations are expected as a result of chemical transformations such as carbon-carbon coupling, heterocyclic ring formation and oxidative dimerization that occur in polyphenols like resveratrol.[29] Bioactivity evaluations of these compounds revealed that the scavengeome of resveratrol represents significantly modulated pharmacological activities when compared to resveratrol. For example, subjecting resveratrol to $ONOO^-$ oxidation (Ox9) resulted in the formation of *trans*-ε- and *trans*-δ-viniferins (**2** and **6**), as well as a nitro-substituted resveratrol (**19**) that collectively resulted in an almost 100% inhibition on ACE at the measured concentration. Other mixtures with high ACE inhibitory action were Ox5 and Ox6, both containing halogen-substituted derivatives. These derivatives also contributed to the modulated inhibitory action on LOX and XO enzymes. Similarly observed, the Fe-catalyzed oxidation of resveratrol led to a mixture containing a variety of minor products (ε- and δ-viniferins and open dimer), with improved lipoxygenase inhibitory activity with resveratrol inactive.[32] Furthermore, Fe-catalysed oxidation of resveratrol in the presence of periodic acid resulted in oxidized mixtures, Ox6 and Ox7, with modulated XO inhibitory activity.

### 5.3 Chemistry of compounds and occurrence in biological environment/systems

The oxidation of resveratrol led to the isolation of a diverse group of compounds, representing a structural diversity that was expectable from our chemical approach. Regarding their biological relevance, it may be particularly noteworthy that compounds **2**, **6** and **16** are expectable products of a resveratrol molecule scavenging free radicals in a biological environment. For instance, chlorine substitution seen in compound **16** may be the result of a reaction of a resveratrol radical with chloride ions, which are abundant in intra- and extracellular fluids. Similarly, the strong self-association of resveratrol via strong $\pi$-$\pi$ stacking in aqueous solution [120] facilitates radical coupling

that could lead to dimers such as **1**, **2**, **4** and **6**, possible in a biological environment under oxidative stress, regardless of the very low concentration of free resveratrol achievable in vivo. Additionally, nitro-derivatives, **18** and **19**, are also expectable products due to the availability of nitric oxide, and its potential to form peroxynitrite in biological systems.[69] To further assess the potential for in vivo formation, resveratrol was oxidized by XO leading to the formation of *trans*-δ-viniferin (**6**), albeit in trace amounts. Given that XO is a ubiquitous enzyme responsible for the oxidation of xanthine and hypoxanthine to uric acid, generating ROS ($O_2^{\bullet-}$ and $H_2O_2$),[106] this finding suggests a plausible biological oxidation pathway. Moreover, activated XO produces significant amounts of superoxide anion in the vascular system under pathophysiological conditions,[106] and, interestingly, the $O_2^{\bullet-}$ scavenging activity of resveratrol is higher in the xanthine/XO system.[66]

Compounds **5**, **12** and **14** are valuable to expand chemical space towards halogen-substituted derivatives related to the biologically more relevant compound **16**. In addition to this, the ethoxy substituted compounds **8–10** are of further interest for their potential formation when resveratrol becomes oxidized in the presence of ethanol, as may occur during the aging of red wine, which is connected to a gradual decline in resveratrol content.[121]

### 5.4 Bioactivity of the isolated compounds

#### 5.4.1 Cardioprotective potential

Numerous studies suggest that cardiovascular diseases (CVDs) like hypertension and cardiac failure are linked to oxidative stress via various signaling pathways in the renin-angiotensin system (RAS).[122,123] An important component of the RAS is the angiotensin-I converting enzyme (ACE), which catalyzes the conversion of angiotensin I to angiotensin II, the primary mediator of the RAS.[124] Angiotensin II stimulates $AT_1$ receptor on smooth muscle cells of the arteriole vasculature causing vasoconstriction and elevation of blood pressure.[125] ACE inhibitors decrease the production of angiotensin II and aldosterone, while simultaneously increasing bradykinin, endothelial NO and prostacyclin, a combined effect that results in vasodilation, and thus cardioprotection.[126]

Resveratrol has shown cardioprotective effects partly through ACE modulation, thereby promoting vascular health.[127] In this study, all tested compounds, except those with a loss of the H-C=C-H, showed greater ACE inhibitory activities than resveratrol, suggesting this bond might be responsible for the activity of natural and semi-synthetic stilbene compounds in inactivating

ACE. Structure–activity relationship analysis revealed that substituting one of the aromatic rings of resveratrol with iodine or chlorine increases the ACE inhibitory effect by approximately 3–12 fold in the order of **16** << **5** < **14** ~ **12**.Consequently, the presence of a 4-iodo group seems more favorable than a 2-iodo group (**12** vs. **5** and **14** vs **5**) in this context, and significantly more favorable than a 2-chloro substitution (**16**). The reduced inhibitory effect of **16** could possibly be a result of the presence and interaction of chlorine with several amino acid acids in the native ACE active site.[77] The presence of these halogenated derivatives in the oxidized mixtures suggest their contribution to the overall activity of these mixtures. Replacing the CH=CH double bond with ethoxy groups, as in **8** and **11**, led to a complete loss of ACE inhibitory activity, regardless of iodine substitution, as observed in **13** and **15**. Nonetheless, ethoxy substitution of the open dimers as in **9** and **10** did not result in such a dramatic loss of activity as that observed in the monomers, **8** and **11**. The most potent ACE inhibitor identified was compound **6**, *trans*-δ-viniferin, a common resveratrol dimer formed from various oxidation models reported, which might explain the improved ACE inhibition of the oxidized mixtures.

ACE comprises two homologous metallopeptidase domains, N and C, joined by a short linker region. While both domains are capable of cleaving the two hemoregulatory peptides angiotensin I and bradykinin, their affinities for substrates and inhibitors differ.[78] The C domain is primarily responsible for angiotensin II production, and hence blood pressure regulation,[128,129] making it a crucial target for antihypertensive drug development. Kinetic studies revealed that compounds **6** and **12** preferentially inhibited the C-domain. The selectivity of ACE inhibitors for either N- or C-domain is controlled by subtle differences in the amino-acids forming the active site.

As **6** was shown to be a competitive inhibitor to the ACE, superimposing the best docked orientation of **6a-**(*R*,*R*) and **6b-**(*S*,*S*) enantiomers with the experimentally bound lisinopril, an approved hypertension drug, in the crystal structure of ACE C- and N-domains (PDB ID: 1O86 and 2C6N, respectively) [77,130] provided important insights into the difference observed between the bioactivities of **6a-(***R,R***)** and **6b-(***S,S***)** as presented in **Figure 2**.

Computational docking analysis showed that **6a-(***R,R***)** has a higher binding affinity to the ACE C-domain than its counterpart **6b-**(*S*,*S*), with affinity values of -10.38 Kcal/mol and -9.9 Kcal/mol, respectively, in their best docked position (**Figure 2A**). The binding orientation of **6a-(***R,R***)** to the active site of C-ACE closely resembles that of lisinopril, which may explain its higher inhibitory potential as compared to its enantiomeric pair, **6b-(***S,S***)**. Zinc, an important catalytic component

of ACE, is bound at the active site to His383, His387 and Glu411,[77] and therefore, the ionic interactions observed between **6a-(*R,R*)** and the residues, Glu411 and Zn701, might provide a structural basis to the inhibitory potential of this compound. Furthermore, several hydrogen bonds were observed between the phenolic hydroxyl groups of **6a-(*R,R*)** and amino acid residues at the active site, notably Arg522 that is essential for chloride activation.[131] Compound **6a-(*R,R*)** also interacted with Glu376 and Val380, recognized as distinct residues contributing to the C-domain selectivity of ACE inhibitors lisW-S, kAW and RXPA380.[129,131] The polar interactions of **6a-(*R,R*)** with Ala354 and His353 are noted to enhance the inhibitory activity of this compound, echoing reported interactions between the pseudo-proline side chain of RXPA380 and the amino acid residues.[131]

In the best docked orientation of both enantiomers in the A subunit of N-ACE as shown in **Figure 2B**, our docking study revealed nearly identical orientation and binding affinities of **6a-(*R,R*)** and **6b-(*S,S*)** in the active site of the N-domain (with a binding energy of -10.02 Kcal/mol and -10.07 Kcal/mol, respectively). Both enantiomers formed several polar and non-polar interactions with the N-domain amino acid residues, similar to those observed in the RXP407 and 33RE [82] but no interaction was observed with Tyr369, which would be crucial for selectivity of the aforementioned N-domain selective inhibitors.[82]

### 5.4.2 Anti-inflammatory activities

Inflammation is central to the development of CVDs, with atherosclerosis serving as an example of a CVD driven by multiple inflammatory mechanisms.[44] Angiotensin II, acting through the AT1 receptor, induces oxidative stress-, which in turn activates several inflammatory mediators, most notably the nuclear factor-κB (NF-κB) pathway, leading to the production of proinflammatory cytokines, TNF-α and IL-6. This cascade further underscores the interconnection between ACE inhibitors and inflammation in cardiovascular disorders.[132-134]

Interdependent of their ability to lower blood pressure, ACE inhibitors may reduce vascular inflammation.[135-137] Thus, several of the oxidized metabolites also had marked anti-inflammatory activities. Benzofuran dimers, along with several open ring dimers, **1** and **9**, had improved LOX inhibition. The presence of an -OH group in **9**, an ethoxy-substituted open ring dimer, seemed to have reversed the observed inactivity of compound **10**, another ethoxy-substituted open ring dimer similar to the compound also reported in the previous study by Shingai and coworkers.[32]

Compounds **9** and **10** may also hold further pharmacological potential, considering that some related stilbene dimers from *Dracaena cochinchinensis* were previously reported as thrombin inhibitory agents.[138] Notably, some iodinated compounds with lower biological relevance (specifically **5** and **12**, with a mono-substitution and **14** with di-substitution, respectively) also exhibited pronounced LOX inhibition. 15-LOX appears to play a crucial role in the development of atherogenesis, and targeting this enzyme could provide a feasible strategy in managing CVDs.[139-141]

Resveratrol has been reported to effectively inhibit cyclooxygenase activity *in vivo* primarily by selectively inhibiting of COX-1 activity and a reducing COX-2 expression at the mRNA level.[142] COX-1 inhibition suppresses thromboxane A2 ($TxA_2$) synthesis, a potent vasoconstrictor and platelet aggregation inducer, thereby mitigating thrombus formation and reducing the risk of myocardial infarction.[143] The importance of inhibiting COX-1 along with antioxidant activity and XO inhibitory potential and its role in cardiovascular protection was thoroughly investigated in 6-gingerol derivatives.[144] Additionally, resveratrol attenuates atherosclerosis-associated inflammation by downregulating COX-2 and its downstream product, prostaglandin E2 (PGE2), a key mediator in arterial inflammation.[145] Most oxidized derivatives obtained in this study were less active COX inhibitors than resveratrol, except for the viniferins **2** and **6**, that showed similar potency. The selective COX-2 inhibition by compound **2** allows for effective anti-inflammatory and analgesic effects while minimizing gastrointestinal side effects typically associated with nonselective NSAIDs.[146]

### 5.4.3 Free Radical Scavenging Activity

Evidence suggests that angiotensin II stimulates NAD(P)H oxidase activation in the arterial wall, a major source of ROS, which then initiates various redox signaling cascades that further amplify oxidative stress such as triggering ROS production by other enzymes such as xanthine oxidase, lipoxygenase and inducible nitric oxide synthase (iNOS).[147-149] The activation of NAD(P)H oxidase and subsequent superoxide generation within the vascular wall plays a pivotal role in atherosclerosis progression and contributes to clinical cardiovascular events.[150] NAD(P)H oxidase-derived superoxide has broader implications for vascular pathology, particularly under inflammatory and oxidative stress conditions, where iNOS activation leads to

an increase in NO production. The resulting NO may react with $O_2^{\bullet-}$ to form peroxynitrite, a highly reactive nitrogen species.[151]

The two antioxidant assays used to determine the antioxidant potential of the oxidized metabolites provide complementary insights since DPPH can be scavenged via hydrogen atom transfer (HAT) or single-electron transfer (SET), whereas the ORAC assay predominantly involves the HAT mechanism.[152] In this study, the DPPH free radical scavenging activity of resveratrol corroborated with some earlier reports,[153,154] and, expectably, we found a potent antioxidant also in the ORAC assay, as reported previously.[155]

Concerning structure–activity relationships based on direct scavenging activity of the compounds, it was observed that substituting one of the aromatic rings with chlorine, as in compound **16**, increased the DPPH scavenging activity, unlike the iodine substitution (**5** and **12**). Iodine substitution, however, significantly increased the compounds' capacity of HAT. Substitution of a phenol ring with electron-donating or electron-withdrawing groups (like halogens) markedly alters the free radical scavenging activity of polyphenols [156] depending on the position and the number of halogen substituents.[157] The presence of halogens have been reported to confer increased potential for HAT,[158] which is in agreement with our results on the iodine-substituted compounds **5** and **12–14**. The ethoxy- substituted dimer **10** had higher TE value than resveratrol, which aligns with similar findings from antioxidant abilities reported for other resveratrol dimers without the benzofuran ring.[159] Notably, several of the oxidized derivatives of resveratrol were found to be similarly or more potent free radical scavengers when compared to their parent compound in either or both bioassays.

In addition to inducing NADPH oxidase, angiotensin II is also known to upregulate xanthine oxidase (XO) expression via ROS and NAD(P)H oxidase activation.[160] Atherosclerosis in humans and experimental animals is associated with increased activity of both endothelial XO and plasma XO,[161,162] suggesting a contribution of XO-derived ROS to cardiovascular disease. In the vascular system, XO produces large amounts of ROS under pathophysiological conditions.[106] XO inhibition is therefore believed to work by reducing the production of ROS that damage blood vessels and contribute to endothelial dysfunction.[163] In addition to reducing oxidative stress, xanthine oxidase inhibitors are reported to reduce cardiovascular risk by reducing uric acid levels. Uric acid is thought to have direct proinflammatory effects on vascular cells, induces inflammation by activating the production of cyclooxygenase 2 (COX2), thromboxane and chemokines.[164,165]

Some metabolites had significantly enhanced ability to inhibit XO compared to resveratrol, as seen in Table 7, with compounds **12** and **16** acting as competitive inhibitors. In the best docked orientation of **12** and **16** in the active site of XO as seen in **Figure 3**, several hydrogen bonds were observed between the phenolic ring containing the two meta-hydroxy groups and several amino acid residues. For both compounds, a hydrogen bond was observed with the molybdopterin residue, Mos1328. Additionally, the halogen substituents of **12** and **16** formed hydrogen bonds with Glu802 and Thr1010, respectively. Proton transfer from the molybdopterin residue's hydroxyl group to Glu1261 is an initial step required for the conversion of xanthine to uric acid by XO, suggesting that the interaction of **16** with this residue is important to the inhibitory effect. Glu802, Arg880, and Thr1010 have also been reported to be essential in the catalytic transformation of xanthine to uric acid.[166,167] Therefore, interactions observed between **12** and **16** and these residues provide a reasonable mechanistic background to the compounds' XO inhibitory activity.[74]

The π–π interactions between the compounds' A-ring and the aromatic ring of residues Phe914 and Phe1009 restricted the compounds to a well-defined plane perpendicular to the base plane of the molybdenum center in the active site, further stabilizing the orientation of both compounds within the XO active site. The orientation and interactions of the hydroxy groups of **12** and **16** are similar to the 5-OH and 7-OH of quercetin and apigenin, both of which are well-studied as XO inhibitors.[85]

### 5.5 In silico evaluation of isolated compounds

Lipinski's Rule of Five (Ro5) serves as a guideline to evaluate the drug-likeness of compounds, focusing on parameters such as molecular weight, lipophilicity (logP), hydrogen bond donors, and acceptors, which can help in predicting their absorption and permeation. Violations of Ro5 parameters can indicate potential challenges in a compound's bioavailability.[168] Increase in molecular weight and logP of a compound reduces its aqueous solubility and membrane permeability, thereby reducing its bioavailability. The Ertl method correlates polar surface area (PSA) with intestinal absorption, indicating that compounds with PSA <60 Å$^2$ are typically well-absorbed, whereas those with PSA >140 Å$^2$ have poor absorption.

Compounds **1**, **10**, and **17**, with PSA values suggesting marginally reduced absorption, may face moderate bioavailability challenges. This aligns with studies on similar polyphenolic

compounds showing that increased PSA can negatively impact oral bioavailability.[169] Aqueous solubility is another critical factor influencing bioavailability, with poor solubility limiting a drug's dissolution rate, thus reducing its absorption and therapeutic efficacy. However, it is important to note that while Ro5 provides a useful framework, there are notable exceptions, especially among certain drug classes like antibiotics and antifungals, which often violate these rules yet remain orally active due to specific structural features or active transport mechanisms.[170] The application of the ligand-lipophilicity efficiency (LLE) metric has proven instrumental in optimizing the balance between potency and lipophilicity during drug development.[171,172] Combining potent inhibitory activity with desirable physicochemical properties revealed compound **6** as a potent and drug-like ACE inhibitor, i.e., a promising agent for cardiovascular protection. Likewise, compounds **2** and **6** were identified as promising LOX inhibitors.

Cytochrome P450 enzymes play a pivotal role in drug metabolism, and inhibition of CYP1A2 can lead to significant drug-drug interactions, affecting the clearance of co-administered drugs metabolized by this enzyme. Similar inhibitory effects have been reported for other polyphenolic compounds, emphasizing the need for comprehensive metabolic studies to assess the safety profiles of these derivatives.[173]

## 6.0 SUMMARY

The aim of this Ph.D. study was to extend the chemical space of oxidized resveratrol derivatives and to examine their pharmacological potential. Our results may be summarized as follows:

**1. Preparation of oxidized resveratrol metabolites.**

A diverse variety of oxidized resveratrol metabolites were prepared after subjecting resveratrol to a variety of oxidants. Based on the metabolic profile diversity and pharmacological investigation to inhibit ACE, LOX, COX-1 and COX-2, and XO, and to exert direct free radical scavenging activity, a total of 19 compounds were isolated, including 7 new compounds.

**2. Biological evaluation of the oxidized derivatives obtained.**

The following results were obtained on the bioactivity of the pure isolated compounds:

- Inhibition of ACE: All compounds except those with a loss of the characteristic H-C=C=H had a better activity than resveratrol. Compound **6** (*trans*-δ-viniferin) was the most potent (20 times more active than resveratrol), and enzyme kinetic and domain-specific studies identified it as a competitive inhibitor, preferentially inhibiting the C-domain of the ACE enzyme by a

selectivity factor of 2.14. Chiral separation and evaluation revealed the **6a-**(*R*,*R*) as the more potent enantiomer in this regard albeit with a relatively low eudysmic ratio of 1.46.

- Inhibition of 15-LOX: While resveratrol was inactive, several of its oxidized derivatives were inhibitors of this enzyme. *Trans*-ε-viniferin (**2**) was the most active compound, followed by its isomer, *trans*-δ-viniferin (**6**)
- Inhibition of COX-1 and COX-2: Similar inhibitory action on COX-1 and COX-2 was observed between resveratrol and several oxidized derivatives. In general, compounds inhibited COX-2 better than COX-1, suggesting that the isolated oxidized metabolites might be more specific to COX-2.
- Inhibition of XO: Compounds **5**, **12** and **16** (all halogen-substituted resveratrol derivatives) were the most potent inhibitors of XO. These compounds also inhibited the enzyme competitively, suggesting that the introduction of a halogen substituent to resveratrol played an important role in interacting with the active site of the enzyme. Resveratrol dimers, *trans*-ε-viniferin (**2**) and *trans*-δ-viniferin (**6**), were also better inhibitors than resveratrol, and were identified as mixed-type inhibitors after enzyme kinetic studies.
- Free radical scavenging potential: With a few of the oxidized derivatives having similar DPPH scavenging potential, compounds exhibited better antioxidant activity by hydrogen atom transfer, evident in the Trolox Equivalent values of the compounds from ORAC assay.
- In silico evaluation: Most of the compounds exhibited physicochemical properties within acceptable parameters. Compounds (**1**, **9**, **10**, **14**, **17**) exhibited violations of Lipinski's Rule of Five (Ro5). *In silico* evaluation of the inhibitory effect on cytochrome P450 1A2 (CyP1A2) isoenzyme revealed comparable potential inhibitory effect for compounds **5**, **18**, and **19**, similar to the inhibition by resveratrol.

In this early-phase drug discovery study, we demonstrated that scavenging various types of biologically relevant ROS/RNS by resveratrol leads to the formation of diverse array of metabolites with enhanced pharmacological activities compared to their parent compound resveratrol itself. As a proof of concept, our approach and findings support a performance-based diversity-oriented exploration of the antioxidant scavengeome as a novel high-hit-rate strategy for drug discovery.

## REFERENCES


(1) Phaniendra, A.; Jestadi, D. B.; Periyasamy, L. Free radicals: properties, sources, targets, and their implication in various diseases. *Indian Journal of Clinical Biochemistry* **2015**, *30* (1), 11-26.

(2) Sies, H.; Jones, D. P. Reactive oxygen species (ROS) as pleiotropic physiological signalling agents. *Nature Reviews Molecular Cell Biology* **2020**, *21* (7), 363-383.

(3) Ruskovska, T.; Maksimova, V.; Milenkovic, D. Polyphenols in human nutrition: from the in vitro antioxidant capacity to the beneficial effects on cardiometabolic health and related inter-individual variability – an overview and perspective. *British Journal of Nutrition* **2020**, *123* (3), 241-254.

(4) Zorov, D. B.; Juhaszova, M.; Sollott, S. J. Mitochondrial reactive oxygen species (ROS) and ROS-induced ROS release. *Physiological Reviews* **2014**, *94* (3), 909-950.

(5) Martemucci, G.; Costagliola, C.; Mariano, M.; D'andrea, L.; Napolitano, P.; D'Alessandro, A. G. Free Radical Properties, Source and Targets, Antioxidant Consumption and Health. *Oxygen* **2022**, *2* (2), 48-78.

(6) Bauer, G. The antitumor effect of singlet oxygen. *Anticancer Research* **2016**, *36* (11), 5649-5663.

(7) Hayyan, M.; Hashim, M. A.; AlNashef, I. M. Superoxide ion: generation and chemical implications. *Chemical Reviews* **2016**, *116* (5), 3029-3085.

(8) Dickinson, B. C.; Chang, C. J. Chemistry and biology of reactive oxygen species in signaling or stress responses. *Nature Chemical Biology* **2011**, *7* (8), 504-511.

(9) Gough, D.; Cotter, T. Hydrogen peroxide: a Jekyll and Hyde signalling molecule. *Cell Death & Disease* **2011**, *2* (10), e213.

(10) Bauer, G. HOCl and the control of oncogenesis. *Journal of Inorganic Biochemistry* **2018**, *179*, 10-23.

(11) Nimse, S. B.; Pal, D. Free radicals, natural antioxidants, and their reaction mechanisms. *RSC Advances* **2015**, *5* (35), 27986-28006.

(12) Pacher, P.; Beckman, J. S.; Liaudet, L. Nitric oxide and peroxynitrite in health and disease. *Physiological Reviews* **2007**, *87* (1), 315-424.

(13) Halliwell, B.; Gutteridge, J. M. *Free Radicals In Biology and Medicine*; Oxford university press, USA, 2015.

(14) Pizzino, G.; Irrera, N.; Cucinotta, M.; Pallio, G.; Mannino, F.; Arcoraci, V.; Squadrito, F.; Altavilla, D.; Bitto, A. Oxidative Stress: Harms and Benefits for Human Health. *Oxidative Medicine and Cellular Longevity* **2017**, *2017*, 8416763.

(15) Halliwell, B. Biochemistry of oxidative stress. *Biochemical Society Transactions* **2007**, *35* (5), 1147-1150.

(16) Birben, E.; Sahiner, U. M.; Sackesen, C.; Erzurum, S.; Kalayci, O. Oxidative Stress and Antioxidant Defense. *World Allergy Organization Journal* **2012**, *5* (1), 9-19.

(17) Forman, H. J.; Zhang, H. Targeting oxidative stress in disease: promise and limitations of antioxidant therapy. *Nature Reviews Drug Discovery* **2021**, *20* (9), 689-709.

(18) Lü, J. M.; Lin, P. H.; Yao, Q.; Chen, C. Chemical and molecular mechanisms of antioxidants: experimental approaches and model systems. *Journal of Cellular and Molecular Medicine* **2010**, *14* (4), 840-860.

(19) Demirci-Çekiç, S.; Özkan, G.; Avan, A. N.; Uzunboy, S.; Çapanoğlu, E.; Apak, R. Biomarkers of Oxidative Stress and Antioxidant Defense. *Journal of Pharmaceutical and Biomedical Analysis* **2022**, *209*, 114477.

(20) Espinosa-Diez, C.; Miguel, V.; Mennerich, D.; Kietzmann, T.; Sánchez-Pérez, P.; Cadenas, S.; Lamas, S. Antioxidant responses and cellular adjustments to oxidative stress. *Redox Biology* **2015**, *6*, 183-197.

(21) Pandey, K. B.; Rizvi, S. I. Plant polyphenols as dietary antioxidants in human health and disease. *Oxidative Medicine and Cellular Longevity* **2009**, *2*, 270-278.

(22) Forman, H. J.; Davies, K. J.; Ursini, F. How do nutritional antioxidants really work: nucleophilic tone and para-hormesis versus free radical scavenging in vivo. *Free Radical Biology and Medicine* **2014**, *66*, 24-35.

(23) Ngo, V.; Duennwald, M. L. Nrf2 and Oxidative Stress: A General Overview of Mechanisms and Implications in Human Disease. *Antioxidants* **2022**, *11* (12), 2345.

(24) Zhou, G.; Myers, R.; Li, Y.; Chen, Y.; Shen, X.; Fenyk-Melody, J.; Wu, M.; Ventre, J.; Doebber, T.; Fujii, N. Role of AMP-activated protein kinase in mechanism of metformin action. *The Journal of Clinical Investigation* **2001**, *108* (8), 1167-1174.
(25) Ji, M.; Gong, X.; Li, X.; Wang, C.; Li, M. Advanced Research on the Antioxidant Activity and Mechanism of Polyphenols from Hippophae Species—A Review. *Molecules*, 2020, 25 (4), 917.
(26) Salisbury, D.; Bronas, U. Reactive oxygen and nitrogen species: impact on endothelial dysfunction. *Nursing Research* **2015**, *64* (1), 53-66.
(27) Luo, J.; Si, H.; Jia, Z.; Liu, D. Dietary Anti-Aging Polyphenols and Potential Mechanisms. *Antioxidants* **2021**, *10* (2), 283.
(28) Hunyadi, A.; Agbadua, O. G., Takács, G,; Balogh, G. T. Scavengome of an Antioxidant. In *Vitamins & Hormones*; Litwack, G., Ed.; Academic Press: Cambridge, MA, USA, **2023**; Vol. 121, pp 81-108.
(29) Hunyadi, A. The mechanism(s) of action of antioxidants: From scavenging reactive oxygen/nitrogen species to redox signaling and the generation of bioactive secondary metabolites. *Medicinal Research Reviews* **2019**, *39* (6), 2505-2533.
(30) Shen, L.; Ji, H.-F. Insights into the inhibition of xanthine oxidase by curcumin. *Bioorganic & Medicinal Chemistry Letters* **2009**, *19* (21), 5990-5993.
(31) Cárcamo, J. M.; Pedraza, A.; Bórquez-Ojeda, O.; Zhang, B.; Sanchez, R.; Golde, D. W. Vitamin C is a kinase inhibitor: dehydroascorbic acid inhibits IκBα kinase β. *Molecular and Cellular Biology* **2004**, *24* (15), 6645-6652.
(32) Shingai, Y.; Fujimoto, A.; Nakamura, M.; Masuda, T. Structure and function of the oxidation products of polyphenols and identification of potent lipoxygenase inhibitors from Fe-catalyzed oxidation of resveratrol. *Journal of Agricultural and Food Chemistry* **2011**, *59* (15), 8180-8186.
(33) Shen, H.; Kannari, K.; Yamato, H.; Arai, A.; Matsunaga, M. Effects of benserazide on L-DOPA-derived extracellular dopamine levels and aromatic L-amino acid decarboxylase activity in the striatum of 6-hydroxydopamine-lesioned rats. *The Tohoku Journal of Experimental Medicine* **2003**, *199* (3), 149-159.
(34) Kourakis, S.; Timpani, C. A.; de Haan, J. B.; Gueven, N.; Fischer, D.; Rybalka, E. Dimethyl fumarate and its esters: a drug with broad clinical utility? *Pharmaceuticals* **2020**, *13* (10), 306.
(35) Arens, A. M.; Shah, K.; Al-Abri, S.; Olson, K. R.; Kearney, T. Safety and effectiveness of physostigmine: a 10-year retrospective review. *Clinical Toxicology* **2018**, *56* (2), 101-107.
(36) Zhang, L.-X.; Li, C.-X.; Kakar, M. U.; Khan, M. S.; Wu, P.-F.; Amir, R. M.; Dai, D.-F.; Naveed, M.; Li, Q.-Y.; Saeed, M. Resveratrol (RV): A pharmacological review and call for further research. *Biomedicine & Pharmacotherapy* **2021**, *143*, 112164.
(37) Prokop, J.; Abrman, P.; Seligson, A. L.; Sovak, M. Resveratrol and Its Glycon Piceid Are Stable Polyphenols. *Journal of Medicinal Food* **2006**, *9* (1), 11-14.
(38) Pannu, N.; Bhatnagar, A. Resveratrol: from enhanced biosynthesis and bioavailability to multitargeting chronic diseases. *Biomedicine & Pharmacotherapy* **2019**, *109*, 2237-2251.
(39) Rauf, A.; Imran, M.; Suleria, H. A. R.; Ahmad, B.; Peters, D. G.; Mubarak, M. S. A comprehensive review of the health perspectives of resveratrol. *Food & Function* **2017**, *8* (12), 4284-4305.
(40) Catalgol, B.; Batirel, S.; Taga, Y.; Ozer, N. K. Resveratrol: French Paradox Revisited. *Frontiers in Pharmacology* **2012**, 3, 141.
(41) Springer, M.; Moco, S. Resveratrol and Its Human Metabolites—Effects on Metabolic Health and Obesity. *Nutrients* **2019**, *11* (1), 143.
(42) Singh, A. P.; Singh, R.; Verma, S. S.; Rai, V.; Kaschula, C. H.; Maiti, P.; Gupta, S. C. Health benefits of resveratrol: Evidence from clinical studies. *Medicinal Research Reviews* **2019**, *39* (5), 1851-1891.
(43) Cheng, H.; Zhang, D.; Wu, J.; Liu, J.; Zhou, Y.; Tan, Y.; Feng, W.; Peng, C. Interactions between gut microbiota and polyphenols: A mechanistic and metabolomic review. *Phytomedicine*, **2023**, 119, 154979.
(44) Baur, J. A.; Sinclair, D. A. Therapeutic potential of resveratrol: the in vivo evidence. *Nature Reviews Drug Discovery* **2006**, *5* (6), 493-506.

(45) Salehi, B.; Mishra, A. P.; Nigam, M.; Sener, B.; Kilic, M.; Sharifi-Rad, M.; Fokou, P. V. T.; Martins, N.; Sharifi-Rad, J. Resveratrol: A double-edged sword in health benefits. *Biomedicines* **2018**, *6* (3), 91.
(46) Elshaer, M.; Chen, Y.; Wang, X. J.; Tang, X. Resveratrol: An overview of its anti-cancer mechanisms. *Life Sciences* **2018**, *207*, 340-349.
(47) Catalgol, B.; Batirel, S.; Taga, Y.; Ozer, N. K. Resveratrol: French paradox revisited. *Frontiers in Pharmacology* **2012**, *3*, 141.
(48) Jang, J. Y.; Im, E.; Kim, N. D. Mechanism of resveratrol-induced programmed cell death and new drug discovery against cancer: a review. *International Journal of Molecular Sciences* **2022**, *23* (22), 13689.
(49) Ferrières, J. The French paradox: lessons for other countries. *Heart* **2004**, *90* (1), 107-111.
(50) Li, H.; Xia, N.; Förstermann, U. Cardiovascular effects and molecular targets of resveratrol. *Nitric Oxide* **2012**, *26* (2), 102-110.
(51) Chu, H.; Li, H.; Guan, X.; Yan, H.; Zhang, X.; Cui, X.; Li, X.; Cheng, M. Resveratrol protects late endothelial progenitor cells from TNF-$\alpha$-induced inflammatory damage by upregulating Krüppel-like factor-2. *Molecular Medicine Reports* **2018**, *17* (4), 5708-5715.
(52) Reuter, S.; Gupta, S. C.; Chaturvedi, M. M.; Aggarwal, B. B. Oxidative stress, inflammation, and cancer: how are they linked? *Free Radical Biology and Medicine* **2010**, *49* (11), 1603-1616.
(53) Meng, T.; Xiao, D.; Muhammed, A.; Deng, J.; Chen, L.; He, J. Anti-Inflammatory Action and Mechanisms of Resveratrol. *Molecules* **2021**, *26* (1), 229.
(54) Gogna, T.; Housden, B. E.; Houldsworth, A. Exploring the Role of Reactive Oxygen Species in the Pathogenesis and Pathophysiology of Alzheimer's and Parkinson's Disease and the Efficacy of Antioxidant Treatment. *Antioxidants* **2024**, *13* (9), 1138.
(55) Andrade, J. M. O.; Barcala-Jorge, A. S.; Batista-Jorge, G. C.; Paraíso, A. F.; de Freitas, K. M.; de Farias Lelis, D.; Guimarães, A. L. S.; de Paula, A. M. B.; Santos, S. H. S. Effect of resveratrol on expression of genes involved thermogenesis in mice and humans. *Biomedicine & Pharmacotherapy* **2019**, *112*, 108634.
(56) Sun, A. Y.; Wang, Q.; Simonyi, A.; Sun, G. Y. Resveratrol as a Therapeutic Agent for Neurodegenerative Diseases. *Molecular Neurobiology* **2010**, *41* (2), 375-383.
(57) Bastianetto, S.; Ménard, C.; Quirion, R. Neuroprotective action of resveratrol. *Biochimica et Biophysica Acta (BBA) - Molecular Basis of Disease* **2015**, *1852* (6), 1195-1201.
(58) Rudrapal, M.; Mishra, A. K.; Rani, L.; Sarwa, K. K.; Zothantluanga, J. H.; Khan, J.; Kamal, M.; Palai, S.; Bendale, A. R.; Talele, S. G.; et al. Nanodelivery of Dietary Polyphenols for Therapeutic Applications. *Molecules* **2022**, *27* (24), 8706.
(59) Xia, N.; Daiber, A.; Förstermann, U.; Li, H. Antioxidant effects of resveratrol in the cardiovascular system. *British Journal of Pharmacology* **2017**, *174* (12), 1633-1646.
(60) Chen, S.; Chen, H.; Du, Q.; Shen, J. Targeting Myeloperoxidase (MPO) Mediated Oxidative Stress and Inflammation for Reducing Brain Ischemia Injury: Potential Application of Natural Compounds. *Frontiers in Physiology* **2020**, 11, 433.
(61) Higashida, K.; Kim, S. H.; Jung, S. R.; Asaka, M.; Holloszy, J. O.; Han, D.-H. Effects of Resveratrol and SIRT1 on PGC-1$\alpha$ Activity and Mitochondrial Biogenesis: A Reevaluation. *PLOS Biology* **2013**, *11* (7), e1001603.
(62) Yang, Y.; Liu, Y.; Wang, Y.; Chao, Y.; Zhang, J.; Jia, Y.; Tie, J.; Hu, D. Regulation of SIRT1 and Its Roles in Inflammation. *Frontiers in Immunology* **2022**, 13, 831168.
(63) Iside, C.; Scafuro, M.; Nebbioso, A.; Altucci, L. SIRT1 Activation by Natural Phytochemicals: An Overview. *Frontiers in Pharmacology* **2020**, 11, 1225.
(64) Yu, C.; Xiao, J.-H. The Keap1-Nrf2 System: A Mediator between Oxidative Stress and Aging. *Oxidative Medicine and Cellular Longevity* **2021**, *2021* (1), 6635460.
(65) Ma, Q. Role of Nrf2 in Oxidative Stress and Toxicity. *Annual Review of Pharmacology and Toxicology* **2013**, *53*, 401-426.

(66) Jia, Z.; Zhu, H.; Misra, B. R.; Mahaney, J. E.; Li, Y.; Misra, H. P. EPR studies on the superoxide-scavenging capacity of the nutraceutical resveratrol. *Molecular and Cellular Biochemistry* **2008**, *313* (1), 187-194.
(67) Dos Santos, A. B.; Santos-Terra, J.; Carletti, J. V.; Deckmann, I.; Gottfried, C. Molecular Alterations in Ferroptosis and the Effects of Resveratrol: A Systematic Review. *Journal of Biochemical and Molecular Toxicology* **2025**, *39* (7), e70384.
(68) Mahal, H.; Mukherjee, T. Scavenging of reactive oxygen radicals by resveratrol: antioxidant effect. *Research on Chemical Intermediates* **2006**, *32* (1), 59-71.
(69) Fási, L.; Latif, A. D.; Zupkó, I.; Lévai, S.; Dékány, M.; Béni, Z.; Könczöl, Á.; Balogh, G. T.; Hunyadi, A. AAPH or Peroxynitrite-Induced Biorelevant Oxidation of Methyl Caffeate Yields a Potent Antitumor Metabolite. *Biomolecules* **2020**, *10* (11), 1537.
(70) Agbadua, O. G.; Kúsz, N.; Berkecz, R.; Vass, E.; Csámpai, A.; Tóth, G.; Balogh, G. T.; Marcourt, L.; Wolfender, J.-L.; Queiroz, E. F.; et al. New Insights into the French Paradox: Free Radical Scavenging by Resveratrol Yields Cardiovascular Protective Metabolites. *Journal of Medicinal Chemistry* **2025**, 68 (10), 10031-10047
(71) Marton, A.; Mohácsi, Z.; Decsi, B.; Csillag, B.; Balog, J.; Schäffer, R.; Karancsi, T.; Balogh, G. T. High-Throughput Drug Stability Assessment via Biomimetic Metalloporphyrin-Catalyzed Reactions Using Laser-Assisted Rapid Evaporative Ionization Mass Spectrometry (LA-REIMS). *Pharmaceutics*, **2024**, 16 (10), 1266.
(72) Ángel Sentandreu, M.; Toldrá, F. A fluorescence-based protocol for quantifying angiotensin-converting enzyme activity. *Nature Protocols* **2006**, *1* (5), 2423-2427.
(73) Quirós, A.; Contreras, M. d. M.; Ramos, M.; Amigo, L.; Recio, I. Stability to gastrointestinal enzymes and structure–activity relationship of β-casein-peptides with antihypertensive properties. *Peptides* **2009**, *30* (10), 1848-1853.
(74) Agbadua, O. G.; Kúsz, N.; Berkecz, R.; Gáti, T.; Tóth, G.; Hunyadi, A. Oxidized Resveratrol Metabolites as Potent Antioxidants and Xanthine Oxidase Inhibitors. *Antioxidants* **2022**, *11* (9), 1832.
(75) Huber, R.; Marcourt, L.; Quiros-Guerrero, L.-M.; Luscher, A.; Schnee, S.; Michellod, E.; Ducret, V.; Kohler, T.; Perron, K.; Wolfender, J.-L.; et al. Chiral Separation of Stilbene Dimers Generated by Biotransformation for Absolute Configuration Determination and Antibacterial Evaluation. *Frontiers in Chemistry* **2022**, 10, No. 912396
(76) Frisch, M. J.; Trucks, G. W.; Schlegel, H. B.; Scuseria, G. E. *Gaussian 16 Rev. C.01*, Wallingford, CT, 2016.
(77) Natesh, R.; Schwager, S. L.; Sturrock, E. D.; Acharya, K. R. Crystal structure of the human angiotensin-converting enzyme–lisinopril complex. *Nature* **2003**, *421* (6922), 551-554.
(78) Corradi, H. R.; Schwager, S. L.; Nchinda, A. T.; Sturrock, E. D.; Acharya, K. R. Crystal structure of the N domain of human somatic angiotensin I-converting enzyme provides a structural basis for domain-specific inhibitor design. *Journal of Molecular Biology* **2006**, *357* (3), 964-974.
(79) Dávid, C. Z.; Kúsz, N.; Agbadua, O. G.; Berkecz, R.; Kincses, A.; Spengler, G.; Hunyadi, A.; Hohmann, J.; Vasas, A. Phytochemical Investigation of Carex praecox Schreb. and ACE-Inhibitory Activity of Oligomer Stilbenes of the Plant. *Molecules* **2024**, *29* (14), 3427.
(80) Caballero, J. Considerations for Docking of Selective Angiotensin-Converting Enzyme Inhibitors. *Molecules*, **2020**, 25, 295.
(81) Xie, D.; Du, L.; Lin, H.; Su, E.; Shen, Y.; Xie, J.; Wei, D. In vitro-in silico screening strategy and mechanism of angiotensin I-converting enzyme inhibitory peptides from α-lactalbumin. *LWT* **2022**, *156*, 112984.
(82) Douglas, R. G.; Sharma, R. K.; Masuyer, G.; Lubbe, L.; Zamora, I.; Acharya, K. R.; Chibale, K.; Sturrock, E. D. Fragment-based design for the development of N-domain-selective angiotensin-1-converting enzyme inhibitors. *Clinical Science* **2014**, *126* (4), 305-313.

(83) O'Boyle, N. M.; Banck, M.; James, C. A.; Morley, C.; Vandermeersch, T.; Hutchison, G. R. Open Babel: An open chemical toolbox. *Journal of Cheminformatics* **2011**, *3* (1), 33.
(84) Duong, N. T.; Vinh, P. D.; Thuong, P. T.; Hoai, N. T.; Thanh, L. N.; Bach, T. T.; Nam, N. H.; Anh, N. H. Xanthine oxidase inhibitors from Archidendron clypearia (Jack.) I.C. Nielsen: Results from systematic screening of Vietnamese medicinal plants. *Asian Pacific Journal of Tropical Medicine* **2017**, *10* (6), 549-556.
(85) Hunyadi, A.; Martins, A.; Danko, B.; Chuang, D.-W.; Trouillas, P.; Chang, F.-R.; Wu, Y.-C.; Falkay, G. Discovery of the first non-planar flavonoid that can strongly inhibit xanthine oxidase: protoapigenone 1′-O-propargyl ether. *Tetrahedron Letters* **2013**, *54* (48), 6529-6532.
(86) Fukumoto, L. R.; Mazza, G. Assessing Antioxidant and Prooxidant Activities of Phenolic Compounds. *Journal of Agricultural and Food Chemistry* **2000**, *48* (8), 3597-3604.
(87) Dávalos, A.; Gómez-Cordovés, C.; Bartolomé, B. Extending Applicability of the Oxygen Radical Absorbance Capacity (ORAC−Fluorescein) Assay. *Journal of Agricultural and Food Chemistry* **2004**, *52* (1), 48-54.
(88) Schmid, R.; Heuckeroth, S.; Korf, A.; Smirnov, A.; Myers, O.; Dyrlund, T. S.; Bushuiev, R.; Murray, K. J.; Hoffmann, N.; Lu, M.; et al. Integrative analysis of multimodal mass spectrometry data in MZmine 3. *Nature Biotechnology* **2023**, *41* (4), 447-449.
(89) Li, S. Y.; Fuchino, H.; Kawahara, N.; Sekita, S.; Satake, M. New Phenolic Constituents from Smilax bracteata. *Journal of Natural Products* **2002**, *65* (3), 262-266.
(90) Panzella, L.; De Lucia, M.; Amalfitano, C.; Pezzella, A.; Evidente, A.; Napolitano, A.; d'Ischia, M. Acid-Promoted Reaction of the Stilbene Antioxidant Resveratrol with Nitrite Ions: Mild Phenolic Oxidation at the 4′-Hydroxystiryl Sector Triggering Nitration, Dimerization, and Aldehyde-Forming Routes. *The Journal of Organic Chemistry* **2006**, *71* (11), 4246-4254.
(91) Lee, H. J.; Seo, J. W.; Lee, B. H.; Chung, K.-H.; Chi, D. Y. Syntheses and radical scavenging activities of resveratrol derivatives. *Bioorganic & Medicinal Chemistry Letters* **2004**, *14* (2), 463-466.
(92) D'Orsi, R.; Morrongiello, F.; Laurita, T.; Funicello, M.; Lupattelli, P.; Chiummiento, L. Regio‐ and Diastereo‐Selective Biomimetic Synthesis of (±)-ε-Viniferin by NIS and Resveratrol. *ChemistrySelect* **2021**, *6* (27), 6863-6866.
(93) Li, X.-Z.; Wei, X.; Zhang, C.-J.; Jin, X.-L.; Tang, J.-J.; Fan, G.-J.; Zhou, B. Hypohalous acid-mediated halogenation of resveratrol and its role in antioxidant and antimicrobial activities. *Food Chemistry* **2012**, *135* (3), 1239-1244.
(94) Predict Molecular Properties | Percepta Software. ACD/Labs. https://www.acdlabs.com/products/percepta-platform/ (accessed July 04, 2023).
(95) Lipinski, C. A.; Lombardo, F.; Dominy, B. W.; Feeney, P. J. Experimental and computational approaches to estimate solubility and permeability in drug discovery and development settings. *Advanced Drug Delivery Reviews* **2012**, *64*, 4-17.
(96) Ertl, P. R., B.; Selzer, P. Calculation of molecular polar surface area as a sum of fragment-based contributions and its application to the prediction of drug transport properties. In *Rational Approaches to Drug Design*, Barcelona, 2001; Höltje, H.-D. S., W., Ed.; Prous: pp 451-455.
(97) Leeson, P. D. Molecular inflation, attrition and the rule of five. *Advanced Drug Delivery Reviews* **2016**, *101*, 22-33.
(98) Leeson, P. D.; Bento, A. P.; Gaulton, A.; Hersey, A.; Manners, E. J.; Radoux, C. J.; Leach, A. R. Target-based evaluation of "drug-like" properties and ligand efficiencies. *Journal of Medicinal Chemistry* **2021**, *64* (11), 7210-7230.
(99) Cotton, J.; Hayashi, M. A.; Cuniasse, P.; Vazeux, G.; Ianzer, D.; De Camargo, A. C.; Dive, V. Selective inhibition of the C-domain of angiotensin I converting enzyme by bradykinin potentiating peptides. *Biochemistry* **2002**, *41* (19), 6065-6071.
(100) Lunow, D.; Kaiser, S.; Rückriemen, J.; Pohl, C.; Henle, T. Tryptophan-containing dipeptides are C-domain selective inhibitors of angiotensin converting enzyme. *Food Chemistry* **2015**, *166*, 596-602.

(101) Mazoir, N.; Benharref, A.; Vaca, L.; Reina, M.; González-Coloma, A. Optimization of Insecticidal Triterpene Derivatives by Biomimetic Oxidations with Hydrogen Peroxide and Iodosobenzene Catalyzed by MnIII and FeIII Porphyrin Complexes. *Chemistry & Biodiversity* **2020**, *17* (9), e2000287.
(102) Kohri, S.; Fujii, H. 2, 2'-Azobis (isobutyronitrile)-derived alkylperoxyl radical scavenging activity assay of hydrophilic antioxidants by employing EPR spin trap method. *Journal of Clinical Biochemistry and Nutrition* **2013**, 13-29.
(103) Yoshida, Y.; Itoh, N.; Saito, Y.; Hayakawa, M.; Niki, E. Application of water-soluble radical initiator, 2, 2′ -azobis-[2-(2-imidazolin-2-yl) propane] dihydrochloride, to a study of oxidative stress. *Free Radical Research* **2004**, *38* (4), 375-384.
(104) Fási, L.; Di Meo, F.; Kuo, C.-Y.; Stojkovic Buric, S.; Martins, A.; Kúsz, N.; Béni, Z.; Dékány, M.; Balogh, G. T.; Pesic, M.; et al. Antioxidant-Inspired Drug Discovery: Antitumor Metabolite Is Formed in Situ from a Hydroxycinnamic Acid Derivative upon Free-Radical Scavenging. *Journal of Medicinal Chemistry* **2019**, *62* (3), 1657-1668.
(105) Fási, L.; Latif, A. D.; Zupkó, I.; Lévai, S.; Dékány, M.; Béni, Z.; Könczöl, Á.; Balogh, G. T.; Hunyadi, A. AAPH or Peroxynitrite-Induced Biorelevant Oxidation of Methyl Caffeate Yields a Potent Antitumor Metabolite. In *Biomolecules*, **2020**, 10 (11), 1537.
(106) Liu, N.; Xu, H.; Sun, Q.; Yu, X.; Chen, W.; Wei, H.; Jiang, J.; Xu, Y.; Lu, W. The role of oxidative stress in hyperuricemia and xanthine oxidoreductase (XOR) inhibitors. *Oxidative Medicine and Cellular Longevity* **2021**, Article1470380.
(107) Ferrer-Sueta, G.; Campolo, N.; Trujillo, M.; Bartesaghi, S.; Carballal, S.; Romero, N.; Alvarez, B.; Radi, R. Biochemistry of Peroxynitrite and Protein Tyrosine Nitration. *Chemical Reviews* **2018**, *118* (3), 1338-1408.
(108) Balazinski, M.; Schmidt-Bleker, A.; Winter, J.; von Woedtke, T. Peroxynitrous Acid Generated In Situ from Acidified H2O2 and NaNO2. A Suitable Novel Antimicrobial Agent? *Antibiotics* **2021**, *10* (8), 1003.
(109) Takahama, U.; Yamamoto, A.; Hirota, S.; Oniki, T. Quercetin-Dependent Reduction of Salivary Nitrite to Nitric Oxide under Acidic Conditions and Interaction between Quercetin and Ascorbic Acid during the Reduction. *Journal of Agricultural and Food Chemistry* **2003**, *51* (20), 6014-6020.
(110) Forman, H. J.; Zhang, H.; Rinna, A. Glutathione: Overview of its protective roles, measurement, and biosynthesis. *Molecular Aspects of Medicine* **2009**, *30* (1), 1-12.
(111) Wang, Y.; Wach, J.-Y.; Sheehan, P.; Zhong, C.; Zhan, C.; Harris, R.; Almo, S. C.; Bishop, J.; Haggarty, S. J.; Ramek, A. Diversity-oriented synthesis as a strategy for fragment evolution against GSK3β. *ACS Medicinal Chemistry Letters* **2016**, *7* (9), 852-856.
(112) Kidd, S. L.; Osberger, T. J.; Mateu, N.; Sore, H. F.; Spring, D. R. Recent Applications of Diversity-Oriented Synthesis Toward Novel, 3-Dimensional Fragment Collections. *Frontiers in Chemistry* **2018**, *6*, 460.
(113) Pavlinov, I.; Gerlach, E. M.; Aldrich, L. N. Next generation diversity-oriented synthesis: a paradigm shift from chemical diversity to biological diversity. *Organic & Biomolecular Chemistry* **2019**, *17* (7), 1608-1623.
(114) Huber, R.; Koval, A.; Marcourt, L.; Héritier, M.; Schnee, S.; Michellod, E.; Scapozza, L.; Katanaev, V. L.; Wolfender, J.-L.; Gindro, K.; et al. Chemoenzymatic Synthesis of Original Stilbene Dimers Possessing Wnt Inhibition Activity in Triple-Negative Breast Cancer Cells Using the Enzymatic Secretome of Botrytis cinerea Pers. *Frontiers in Chemistry* **2022**, 10, Article 881298
(115) Huber, R.; Marcourt, L.; Héritier, M.; Luscher, A.; Guebey, L.; Schnee, S.; Michellod, E.; Guerrier, S.; Wolfender, J.-L.; Scapozza, L. Generation of potent antibacterial compounds through enzymatic and chemical modifications of the trans-δ-viniferin scaffold. *Scientific Reports* **2023**, *13* (1), 15986.
(116) Righi, D.; Huber, R.; Koval, A.; Marcourt, L.; Schnee, S.; Le Floch, A.; Ducret, V.; Perozzo, R.; de Ruvo, C. C.; Lecoultre, N. Generation of stilbene antimicrobials against multiresistant strains of Staphylococcus aureus through biotransformation by the enzymatic secretome of Botrytis cinerea. *Journal of Natural Products* **2020**, *83* (8), 2347-2356.

(117) Galloway, W. R. J. D.; Wilcke, D.; Nie, F.; Hadje-Georgiou, K.; Laraia, L.; Spring, D. R. Diversity-Oriented Synthesis: Developing New Chemical Tools to Probe and Modulate Biological Systems. In *Concepts and Case Studies in Chemical Biology*, 2014; pp 379-390.
(118) Galloway, W. R. J. D.; Isidro-Llobet, A.; Spring, D. R. Diversity-oriented synthesis as a tool for the discovery of novel biologically active small molecules. *Nature Communications* **2010**, *1* (1), 80.
(119) Karlsson, J.; Emgard, M.; Brundin, P.; Burkitt, M. J. trans‐Resveratrol Protects Embryonic Mesencephalic Cells from tert‐Butyl Hydroperoxide: Electron Param. *Journal of Neurochemistry* **2000**, *75* (1), 141-150.
(120) Velu, S. S.; Di Meo, F.; Trouillas, P.; Sancho-Garcia, J.-C.; Weber, J.-F. F. Regio-and stereocontrolled synthesis of oligostilbenoids: Theoretical highlights at the supramolecular level. *Journal of Natural Products* **2013**, *76* (4), 538-546.
(121) Naiker, M.; Anderson, S.; Johnson, J.; Mani, J.; Wakeling, L.; Bowry, V. Loss of trans‐resveratrol during storage and ageing of red wines. *Australian Journal of Grape and Wine Research* **2020**, *26* (4), 385-387.
(122) Fanelli, C.; Zatz, R. Linking Oxidative Stress, the Renin-Angiotensin System, and Hypertension. *Hypertension* **2011**, *57* (3), 373-374..
(123) Landmesser, U.; Drexler, H. Oxidative stress, the renin-angiotensin system, and atherosclerosis. *European Heart Journal Supplements* **2003**, 5 (Suppl A), A3 -A7.
(124) Polakovičová, M.; Jampílek, J. Advances in structural biology of ACE and development of domain selective ACE-inhibitors. *Medicinal Chemistry* **2019**, *15* (6), 574-587.
(125) Patten, G. S.; Abeywardena, M. Y.; Bennett, L. E. Inhibition of angiotensin converting enzyme, angiotensin II receptor blocking, and blood pressure lowering bioactivity across plant families. *Critical Reviews in Food Science and Nutrition* **2016**, *56* (2), 181-214.
(126) Royster, R. L.; Groban, L.; Locke, A. Q.; Morris, B. N.; Slaughter, T. F. Chapter 8 - Cardiovascular Pharmacology. In *Kaplan's Essentials of Cardiac Anesthesia (Second Edition)*, Kaplan, J. A. Ed.; Elsevier, **2018**; pp 132-166.
(127) Ma, E.; Wu, C.; Chen, J.; Wo, D.; Ren, D.-n.; Yan, H.; Peng, L.; Zhu, W. Resveratrol prevents Ang II-induced cardiac hypertrophy by inhibition of NF-κB signaling. *Biomedicine & Pharmacotherapy* **2023**, *165*, 115275.
(128) Fuchs, S.; Xiao, H. D.; Hubert, C.; Michaud, A.; Campbell, D. J.; Adams, J. W.; Capecchi, M. R.; Corvol, P.; Bernstein, K. E. Angiotensin-converting enzyme C-terminal catalytic domain is the main site of angiotensin I cleavage in vivo. *Hypertension* **2008**, *51* (2), 267-274.
(129) Watermeyer, J. M.; Kroeger, W. L.; O'Neill, H. G.; Sewell, B. T.; Sturrock, E. D. Characterization of domain-selective inhibitor binding in angiotensin-converting enzyme using a novel derivative of lisinopril. *Biochemical Journal* **2010**, *428* (1), 67-74.
(130) Wei, L.; Alhenc-Gelas, F.; Corvol, P.; Clauser, E. The two homologous domains of human angiotensin I-converting enzyme are both catalytically active. *Journal of Biological Chemistry* **1991**, *266* (14), 9002-9008.
(131) Georgiadis, D.; Cuniasse, P.; Cotton, J.; Yiotakis, A.; Dive, V. Structural determinants of RXPA380, a potent and highly selective inhibitor of the angiotensin-converting enzyme C-domain. *Biochemistry* **2004**, *43* (25), 8048-8054.
(132) Fanelli, C.; Zatz, R. Linking oxidative stress, the renin-angiotensin system, and hypertension. *Hypertension* **2011**, 57, 373-374.
(133) Rincón, J.; Correia, D.; Arcaya, J.; Finol, E.; Fernández, A.; Pérez, M.; Yaguas, K.; Talavera, E.; Chávez, M.; Summer, R. Role of Angiotensin II type 1 receptor on renal NAD (P) H oxidase, oxidative stress and inflammation in nitric oxide inhibition induced-hypertension. *Life Sciences* **2015**, *124*, 81-90.
(134) Dandona, P.; Dhindsa, S.; Ghanim, H.; Chaudhuri, A. Angiotensin II and inflammation: the effect of angiotensin-converting enzyme inhibition and angiotensin II receptor blockade. *Journal of Human Hypertension* **2007**, *21* (1), 20-27.

(135) Montecucco, F.; Pende, A.; Mach, F. The renin-angiotensin system modulates inflammatory processes in atherosclerosis: evidence from basic research and clinical studies. *Mediators of Inflammation* **2009**, *2009*.
(136) da Cunha, V.; Tham, D. M.; Martin-McNulty, B.; Deng, G.; Ho, J. J.; Wilson, D. W.; Rutledge, J. C.; Vergona, R.; Sullivan, M. E.; Wang, Y.-X. J. Enalapril attenuates angiotensin II-induced atherosclerosis and vascular inflammation. *Atherosclerosis* **2005**, *178* (1), 9-17.
(137) Mu̇nzel, T.; Keaney Jr, J. F. Are ACE inhibitors a "magic bullet" against oxidative stress? *Circulation* **2001**, *104* (13), 1571-1574.
(138) Zhu, Y.; Zhang, P.; Yu, H.; Li, J.; Wang, M.-W.; Zhao, W. Anti-Helicobacter pylori and Thrombin Inhibitory Components from Chinese Dragon's Blood, Dracaena cochinchinensis. *Journal of Natural Products* **2007**, *70* (10), 1570-1577.
(139) Kayama, Y.; Minamino, T.; Toko, H.; Sakamoto, M.; Shimizu, I.; Takahashi, H.; Okada, S.; Tateno, K.; Moriya, J.; Yokoyama, M. Cardiac 12/15 lipoxygenase–induced inflammation is involved in heart failure. *Journal of Experimental Medicine* **2009**, *206* (7), 1565-1574.
(140) Liu, T.; Ai, D. Roles of Lipoxygenases in Cardiovascular Diseases. *Journal of Cardiovascular Translational Research* **2025**, *18* (3), 599-610.
(141) Kong, P.; Cui, Z.-Y.; Huang, X.-F.; Zhang, D.-D.; Guo, R.-J.; Han, M. Inflammation and atherosclerosis: signaling pathways and therapeutic intervention. *Signal Transduction and Targeted Therapy* **2022**, *7* (1), 131.
(142) Kanduja, K. L.; Hardwaj, A.; Kaushik, G. Resveratrol inhibits N-nitrosodiethylamine-induced ornithine decarboxylase and cyclooxygenase in mice. *Journal of Nutritional Science and Vitaminology* **2004**, *50* (1), 61-65.
(143) Wang, Z.; Huang, Y.; Zou, J.; Cao, K.; Xu, Y.; Wu, J. M. Effects of red wine and wine polyphenol resveratrol on platelet aggregation in vivo and in vitro. *International Journal of Molecular Medicine* **2002**, *9* (1), 77-79.
(144) Ahmed, S. H. H.; Gonda, T.; Agbadua, O. G.; Girst, G.; Berkecz, R.; Kúsz, N.; Tsai, M.-C.; Wu, C.-C.; Balogh, G. T.; Hunyadi, A. Preparation and Evaluation of 6-Gingerol Derivatives as Novel Antioxidants and Antiplatelet Agents. *Antioxidants* **2023**, *12* (3), 744.
(145) Harikumar, K. B.; Aggarwal, B. B. Resveratrol: a multitargeted agent for age-associated chronic diseases. *Cell Cycle* **2008**, *7* (8), 1020-1035.
(146) Shi, S.; Klotz, U. Clinical use and pharmacological properties of selective COX-2 inhibitors. *European Journal of Clinical Pharmacology* **2008**, *64*, 233-252.
(147) Shi, X.; Guan, Y.; Jiang, S.; Li, T.; Sun, B.; Cheng, H. Renin-angiotensin system inhibitor attenuates oxidative stress induced human coronary artery endothelial cell dysfunction via the PI3K/AKT/mTOR pathway. *Archives of Medical Science* **2019**, *15* (1), 152-164, journal article.
(148) Wojewodzka-Zelezniakowicz, M.; Gromotowicz-Poplawska, A.; Kisiel, W.; Konarzewska, E.; Szemraj, J.; Ladny, J. R.; Chabielska, E. Angiotensin-converting enzyme inhibitors attenuate propofol-induced pro-oxidative and antifibrinolytic effect in human endothelial cells. *Journal of the Renin-Angiotensin-Aldosterone System* **2017**, *18* (1), 1470320316687197.
(149) Manucha, W.; Ritchie, B.; Ferder, L. Hypertension and insulin resistance: implications of mitochondrial dysfunction. *Current Hypertension Reports* **2015**, *17*, 1-7.
(150) Moris, D.; Spartalis, M.; Spartalis, E.; Karachaliou, G.-S.; Karaolanis, G. I.; Tsourouflis, G.; Tsilimigras, D. I.; Tzatzaki, E.; Theocharis, S. The role of reactive oxygen species in the pathophysiology of cardiovascular diseases and the clinical significance of myocardial redox. *Annals of Translational Medicine* **2017**, *5* (16).
(151) Lubos, E.; Handy, D. E.; Loscalzo, J. Role of oxidative stress and nitric oxide in atherothrombosis. *Frontiers in Bioscience: A Journal and Virtual Library* **2008**, *13*, 5323-5344.
(152) Liang, N.; Kitts, D. D. Antioxidant Property of Coffee Components: Assessment of Methods that Define Mechanisms of Action. *Molecules* **2014**, *19* (11), 19180-19208.

(153) Gülçin, İ. Antioxidant properties of resveratrol: A structure–activity insight. *Innovative Food Science & Emerging Technologies* **2010**, *11* (1), 210-218.
(154) Lin, J.; Li, X.; Chen, B.; Wei, G.; Chen, D. E-Configuration Improves Antioxidant and Cytoprotective Capacities of Resveratrols. *Molecules*, **2018**, 23 (7), 1790.
(155) Intagliata, S.; Spadaro, A.; Lorenti, M.; Panico, A.; Siciliano, E. A.; Barbagallo, S.; Macaluso, B.; Kamble, S. H.; Modica, M. N.; Montenegro, L. In Vitro Antioxidant and Anti-Glycation Activity of Resveratrol and Its Novel Triester with Trolox. *Antioxidants*, **2021**, 10 (1), 12.
(156) Lee, C. Y.; Nanah, C. N.; Held, R. A.; Clark, A. R.; Huynh, U. G. T.; Maraskine, M. C.; Uzarski, R. L.; McCracken, J.; Sharma, A. Effect of electron donating groups on polyphenol-based antioxidant dendrimers. *Biochimie* **2015**, *111*, 125-134.
(157) Lee, C. Y.; Sharma, A.; Semenya, J.; Anamoah, C.; Chapman, K. N.; Barone, V. Computational Study of Ortho-Substituent Effects on Antioxidant Activities of Phenolic Dendritic Antioxidants. *Antioxidants*, **2020**, 9 (3), 189.
(158) Capaldo, L.; Ravelli, D. Hydrogen Atom Transfer (HAT): A Versatile Strategy for Substrate Activation in Photocatalyzed Organic Synthesis. *European Journal of Organic Chemistry* **2017**, *2017* (15), 2056-2071.
(159) Li, C.; Xu, X.; Tao, Z.; Wang, X. J.; Pan, Y. Resveratrol dimers, nutritional components in grape wine, are selective ROS scavengers and weak Nrf2 activators. *Food Chemistry* **2015**, *173*, 218-223.
(160) Landmesser, U.; Spiekermann, S.; Preuss, C.; Sorrentino, S.; Fischer, D.; Manes, C.; Mueller, M.; Drexler, H. Angiotensin II induces endothelial xanthine oxidase activation: role for endothelial dysfunction in patients with coronary disease. *Arteriosclerosis, Thrombosis, and Vascular Biology* **2007**, *27* (4), 943-948.
(161) Guzik, T. J.; Sadowski, J.; Guzik, B.; Jopek, A.; Kapelak, B.; Przybyłowski, P.; Wierzbicki, K.; Korbut, R.; Harrison, D. G.; Channon, K. M. Coronary artery superoxide production and nox isoform expression in human coronary artery disease. *Arteriosclerosis, Thrombosis, and Vascular Biology y* **2006**, *26* (2), 333-339.
(162) Polito, L.; Bortolotti, M.; Battelli, M. G.; Bolognesi, A. Xanthine oxidoreductase: A leading actor in cardiovascular disease drama. *Redox Biology* **2021**, *48*, 102195.
(163) Mudgal, R.; Singh, S. Xanthine oxidoreductase in the pathogenesis of endothelial dysfunction: An update. *Current Hypertension Reviews* **2024**, *20* (1), 10-22.
(164) Saito, H.; Tanaka, K.; Iwasaki, T.; Oda, A.; Watanabe, S.; Kanno, M.; Kimura, H.; Shimabukuro, M.; Asahi, K.; Watanabe, T. Xanthine oxidase inhibitors are associated with reduced risk of cardiovascular disease. *Scientific Reports* **2021**, *11* (1), 1380.
(165) Borghi, C.; Agabiti-Rosei, E.; Johnson, R. J.; Kielstein, J. T.; Lurbe, E.; Mancia, G.; Redon, J.; Stack, A. G.; Tsioufis, K. P. Hyperuricaemia and gout in cardiovascular, metabolic and kidney disease. *European Journal of Internal Medicine* **2020**, *80*, 1-11.
(166) Cao, H.; Pauff, J. M.; Hille, R. Substrate Orientation and Catalytic Specificity in the Action of Xanthine Oxidase: The sequential hydroxylation of hypoxanthine to uric acid. *Journal of Biological Chemistry* **2010**, *285* (36), 28044-28053.
(167) Ribeiro, P. M. G.; Fernandes, H. S.; Maia, L. B.; Sousa, S. F.; Moura, J. J. G.; Cerqueira, N. M. F. S. A. The complete catalytic mechanism of xanthine oxidase: a computational study. *Inorganic Chemistry Frontiers* **2021**, *8* (2), 405-416.
(168) Roskoski Jr, R. Rule of five violations among the FDA-approved small molecule protein kinase inhibitors. *Pharmacological Research* **2023**, *191*, 106774.
(169) Stefaniu, A.; Pirvu, L. C. In silico study approach on a series of 50 polyphenolic compounds in plants; A comparison on the bioavailability and bioactivity data. *Molecules* **2022**, *27* (4), 1413.
(170) Doak, Bradley C.; Over, B.; Giordanetto, F.; Kihlberg, J. Oral Druggable Space beyond the Rule of 5: Insights from Drugs and Clinical Candidates. *Chemistry & Biology* **2014**, *21* (9), 1115-1142.
(171) Johnson, T. W.; Gallego, R. A.; Edwards, M. P. Lipophilic efficiency as an important metric in drug design. *Journal of Medicinal Chemistry* **2018**, *61* (15), 6401-6420.

(172) Gallego, R. A.; Edwards, M. P.; Montgomery, T. P. An update on lipophilic efficiency as an important metric in drug design. *Expert Opinion on Drug Discovery* **2024**, *19* (8), 917-931.
(173) Buyukyildirim, T.; Senol Deniz, F. S.; Tugay, O.; Salmas, R. E.; Ulutas, O. K.; Aysal, I. A.; Orhan, I. E. Chromatographic Analysis and Enzyme Inhibition Potential of Reynoutria japonica Houtt.: Computational Docking, ADME, Pharmacokinetic, and Toxicokinetic Analyses of the Major Compounds. *Pharmaceuticals* **2025**, *18* (3), 408.

**ACKNOWLEDGEMENT**

First and foremost, I would like to express my most profound and deepest appreciation to my supervisor, Prof. Attila Hunyadi, for his mentoring, supervision, and encouragement during my Ph.D. study. His immense knowledge, contributions, and guidance helped me sieve through the various challenges that occurred. I am deeply indebted to him.

Secondly, I am thankful to Prof. Dr. Judit Hohmann, the Head of Doctoral School of Pharmaceutical Sciences, and who was the Head of the Institute of Pharmacognosy, at the beginning of my studies. She provided an extremely conducive environment, and her advice and support were important in my study.

I wish to thank all co-authors who contributed their professional expertise. I am grateful to Dr. Norbert Kúsz, Prof. Dr. Gábor Tóth and Dr. Tamás Gáti for the NMR investigations. I am also grateful to Dr. Róbert Berkecz for the assistance provided in the HR-MS measurements. I extend my appreciation to Dr. Emerson Ferreira Queiroz, Prof. Jean-Luc Wolfender, Dr. Laurence Marcourt and Dr. Robin Huber for their contributions towards metabolomic profiling of the oxidized mixtures and pure compounds. I wish to thank Prof. György Tibor Balogh for his help with *in silico* evaluation of the compounds for drug likeness. In addition to helping with this evaluation, I wish to thank him along with Andras Marton and Tamás Karancsi for their help with LA-REIMS measurements. I finally wish to appreciate Dr. Elemér Vass and Prof. Antal Csámpai for their assistance in VCD and absolute configuration determination.

I thank Dr. Meriem Issaadi for taking me under her wing when I first arrived at the department. I owe special thanks to Ibolya Hevérné Herke for her selflessness and her assistance daily during my research work. I appreciate Dr. Gábor Girst for his help with plate reader measurements. I am especially thankful to other past and current members of the Natural Product Chemical Space Research Group, Institute of Pharmacognosy, University of Szeged.

I wish to thank all members of the Institute of Pharmacognosy for the friendly, wonderful and supportive atmosphere provided during these years. It made my research less tedious and provided me with strength to perform daily tasks needed to complete my study.

Special thanks to the members of my wife, Peace; my brother, Eshi and his family, Jemi, Nathan and Justin; and most importantly, to my mother, whose sacrifice, prayer and encouragement guided me throughout my Ph.D. studies. I am thankful to the Ugbodagas, for their continued love and support. I express my gratitude to the Omamulis for their love and kindness. I am deeply grateful to every family member and friend back in Nigeria for their continued support and encouragement.

I also extend my sincere thanks to all my friends, football and basketball teammates, and everyone I met in Hungary during my program. Their daily encouragement and love strengthened me.

Lastly, I acknowledge the funding provided by the National Research, Development and Innovation Office, Hungary (NKFIH; K119770 and K109293), and TKP2021-EGA-32, implemented with the support provided by the Ministry of Innovation and Technology of Hungary from the NKFIH, financed under the TKP2021-EGA funding scheme. I am also thankful to the Tempus Public Foundation of the Hungarian government for the Stipendium Hungaricum Scholarship and the Bilateral Education Agreement (BEA) Scholarship of the Nigerian government.